A Thesis

On

Study of structural, thermal and ionic conductivity of $(1-x)Bi_2O_3.xTiO_2$ $(0.05 \leq x \leq 0.20)$ systems

Submitted in the partial fulfillment of requirement for the Degree of

Master of Technology

in

Materials and Metallurgical Engineering

By

Gourav Singla

Roll No.-600802006

Under the supervision of

Dr. Kulvir Singh

Associate Professor

School of Physics and Materials Science

Thapar University, Patiala (Punjab)

July-2010

Dedicated
to
My Loving Parents

CERTIFICATE

This is to certify that the thesis entitled **"Study of structural, thermal and ionic conductivity of (1-x)Bi_2O_3.xTiO_2 (0.05≤x≤0.20) systems"** submitted by **Gourav Singla** in the partial fulfillment of the requirement for the award of the degree of **M. Tech** in **Materials and Metallurgical Engineering** from the School of Physics and Materials Science, Thapar University, Patiala, is a record of candidate's own work carried out by him under my supervision and guidance. The matter embodied in this report has not been submitted in part or full to any other University or institute for the award of any degree.

(Dr. Kulvir Singh)

Associate Professor

School of Physics and Materials Science

Countersigned by:

(Dr. O.P. Pandey)

Professor and Head, SPMS

Thapar University

Patiala, Punjab (147004)

(Dr. R.K Sharma)

Dean, Academic Affairs

Thapar University

Patiala, Punjab (147004)

ACKNOWLEDGEMENTS

I express my deep gratitude and respects to my guide **Dr. Kulvir Singh** for his keen interest and valuable guidance, strong motivation and constant encouragement during the course of the work. I thank him for his great patience, constructive criticism and myriad useful suggestions apart from invaluable guidance to me.

I am grateful to **Dr. O.P. Pandey, Professor and Head, School of Physics and Materials Science** for his encouragement and execution of thesis work.

No task is single man's effort. Various factors, situations and persons integrate to provide the background for the accomplishment of a task. Foremost, I'm indebted to God almighty that has been there today and always.

My project would not have seen daylight without the immense cooperation of **Ms. Jasmeet Gill (Research scholar)** who helped me at various stages during the due course of my work.

I would like to thanks **Mr. Vishal Kumar, Mr. Akshay, Mr. Ravi Sukhla, Mr. Kapil Sood**, **Ms. Kamalpreet, Mrs. Bhupinder Kaur, Mrs. Gurbinder** and all other **Phd. scholars** in the department without whom the project work not have been possible.

My sincere thanks to **Mr. Purushotam** for his help to carry out X-Ray diffraction studies and SEM.

The help provided by **S. Jant Singh** is highly acknowledged.

I am greatful to my friends **Param, Rashmi, Ram and Ritesh** for their cooperation and support.

I owe my sincere thanks to all the staff members of **School of Physics and Materials Science** for their support and encouragement.

Last but not the least; I would like to thank my **parents** for their moral support that kept my spirit up during the endeavor.

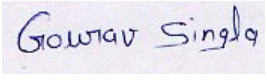

Gaurav Singla

Contents

List of Symbols and Abbreviations

SOFC	Solid Oxide Fuel Cell
^{o}C	Degree Celsius
BASE	Beta-alumina solid electrolyte
β"	Beta prime-prime
PEM	Polymer Electrolyte membrane
MEA	Membrane Electrode assembly
σ	Conductivity
P	Methanol Permeability
PWA	Phosphotungstic acid
YSZ	Yttria-stabilized zirconia
IT-SOFC	Intermediate Temperature SOFC
δ	Delta
α	Alpha
γ	Gamma
β	Beta
μm	Micro metre

kb	Kilo Byte
AC	Alternating Current
XRD	X-ray Diffraction
DTA	Differential Thermal Analysis
DSC	Differential Scanning Calorimetry
SEM	Scanning Electron Microscopy
DC	Direct Current

List of Figures

List of Tables

Abstract

Solid electrolytes are very important and essential part of solid oxide fuel cells. The Y_2O_3 stabilized ZrO_2 (YSZ) are being used as a electrolyte in SOFCs. However, the ionic conductivity of YSZ drastically decreases below 1000 ºC. In all over the world, the efforts are being made to reduce the working temperature of SOFC for making them commercially viable. Therefore, in the present study, titanium-substituted compounds ($Bi_{2-x}Ti_xO_{3+x/2}$ $0.05 \leq x \leq 0.20$) were prepared by solid-state reaction technique for its use as an electrolyte in SOFC. Structural and conductivity behavior was studied as a function of the Ti^{4+} substitution on bismuth site. The as prepared samples were studied by using alternating current conductivity, differential thermal analysis, SEM and X-ray diffraction techniques. The XRD results indicate the formation of Cubic $Bi_{12}TiO_{20}$ phase. Apart from this, Bi_2O_3 are also identified as minority phase in all the samples. The volume fraction of $Bi_{12}TiO_{20}$ phase increses with increasing concentration of TiO_2 with decreasing minority phase Bi_2O_3. The highest ionic conductivity was observed in x=0.15 sample. The results are discussed in light of disordering and lower polarizability of Ti^{4+} cation as compared to Bi^{3+} cation.

Chapter 1

Introduction

1.1 Background

The modern scientific and technological approach, in the area of energy production, is to develop inexpensive devices which could satisfy the current drive for cleaner and more efficiently distributed power. Fuel cells represent a promising and viable alternative for large scale generation of electricity, with minimal undesirable chemical, thermal and acoustic emissions. A fuel cell is a device that directly converts the chemical energy of reactants (a fuel such as hydrogen, natural gas, methane or methanol and an oxidant air or oxygen) into electricity. Solid Oxide Fuel Cell (SOFC) is the most advancing field in the science of fuel cell due to its higher efficiency as compared to other fuel cells operates in the vicinity of temperature of 800 ^{o}C-1000 ^{o}C. The obstacle in the commercialization of SOFCs is their high operating temperature. The fuel cell operating temperature mostly depends on the choice of the electrolyte material. Thus the choice of the electrolyte material, conductivity, stability and the availability of suitable techniques for fabrication of thin films become critical issues in consideration of the lower temperature operation. Solid electrolyte is the important part of SOFCs. The electrolyte for SOFC must be stable in both reducing and oxidizing conditions and must have sufficiently high ionic conductivity with low electronic conductivity at the cell operating temperature. Until, now stabilised zirconia especially yttria stabilised zirconia possessing the fluorite structure has been the most favoured electrolyte for SOFCs.

Other fluorite structure oxide ion conductor such as doped ceria has also been proposed as the electrolyte material for SOFCs due to its good ionic conductivity in lower temperature range (600 ^{o}C-800 ^{o}C). More recently a number of other materials have found to possess good ionic conductivity and several efforts have also been made to develop a suitable solid electrolyte which has higher ionic conductivity in intermediate temperature range (600 ^{o}C-800 ^{o}C).

1.2 Ionic conductors

The substance in which ionic conduction takes place through movement of ions is called ionic conductor. Ionic conductivity is observed in those solids in which defects (vacancies) exist. Ionic conductors have always provided a fascinating interdisciplinary field of study ever since their discovery by Faraday over 200 years ago. He introduced the basic terminology of electrochemistry and classification of substances into first and second type of conductors in 1834. In 1897, Nernst suggested that a solid electrolyte in the form of thin rod could be made electrically conducting and then kept glowing by the passage of an electric current. Later investigation led to his observation that the conductivity of pure oxide rise very slowly with temperature and remains relatively low, whereas mixture possess an enormously much greater conductivity. The empirical phase of the development of solid electrolyte was overcome after many general advances in research on solids. These included development of X-ray structure analysis, new knowledge on the ion conduction of solids from the measurement of transport numbers, the establishment of the theory of disorder in solids and the development of isotope method for the investigation of diffusion processes in solids. In recent years, solid ionic conductors are widely used in batteries, fuel cells and other large and small devices etc. The ionic conductivity is a critical property of a solid electrolyte which determines the efficiency and operating temperature of electrochemical cells. In order to obtain a material that is a pure ion conductor (solid electrolyte), the level of electronic contribution to the total electrical conductivity (ionic + electronic) must be negligible. Solid electrolyte must have high ionic conductivity at the operating temperature to allow efficient transfer of ions from the cathode to anode and also a low electronic conductivity.

1.3 Solid Electrolytes: Classification

Oxide ion conductors are a class of materials in which oxide ion migrate through the crystal framework formed by the cation sublattice. This usually occurs via a series of “hops” between adjacent, equivalent sites in the oxide ion sublattice, due to the presence of vacancies. The magnitude of the conductivity is dependent on the concentration of vacancies, the number of possible hopping paths, and the interaction of oxide ions with the immobiles cation sublattice.

Solid compounds that exhibit the high ionic conductivity are termed as solid electrolytes or superionic conductors or fast ion conductors or hyperionic conductors. Solid electrolytes have either mobile anions or cations, which due to their high degree of disorder are free to move throughout the structure. The maximum ionic conductivity of these materials lies between 0.1 and 10 ohm^{-1} cm^{-1}.

There are a number of different types of oxide ion conductive solid electrolyte materials, both in terms of chemical composition and crystal structure. These include Bi_2O_3–based materials $Bi_{0.70}Sr_{0.30}O_{1.35}$ with a rhombohedral structure [1] and layered BIMEVOX materials such as $Bi_2V_{0.9}Cu_{0.1}O_{5.35}$ [2]. Different solid electrolytes can be broadly categorized as follows:

1.3.1 Beta-alumina Solid Electrolyte

Beta-alumina solid electrolyte (BASE) is a fast ion conductor material used as a membrane in several types of molten salt electrochemical cell. There is no known substitute.

β"-Alumina (*beta prime-prime alumina*) is an isomorphic form of aluminium oxide (Al_2O_3) a hard polycrystalline ceramic which when prepared as an electrolyte is complexed with a mobile ion, such as Na^+, K^+ , Li^+ , Ag^+ , H^+ , Pb^{2+} , Sr^{2+} or Ba^{2+} depending on the application. Beta-alumina is a good conductor of its mobile ion yet allows no non-ionic (i.e. electronic) conductivity.

Sodium beta alumina is a non-stoichiometric sodium aluminate known for its rapid transport of Na^+ ions. This material selectively passes sodium ions while blocking other species, including liquid sodium and liquid sulfur. It is a ceramic which can be formed and sintered by commercially available techniques and its conductivity at operating temperatures 250 ^oC to 300 ^oC compares favorably with electrolytes used in conventional battery systems such as sulfuric acid and potassium hydroxide. The crystal structure of the Na-Al_2O_3 provides an essential rigid framework with channels along which the ionic species of the solid can migrate. Ion transport involves hopping from site to site along these channels.

1.3.2 Polymer Electrolyte Membrane

A polymer electrolyte membrane (PEM) or proton exchange membrane is a semipermeable membrane generally made from ionomers and designed to conduct protons while being impermeable to gases such as oxygen or hydrogen. This is their essential function when incorporated into a membrane electrode assembly (MEA) of a proton exchange membrane fuel cell or of a proton exchange membrane electrolyser: separation of reactants and transport of protons.

PEMs can be made from either pure polymer membranes or from composite membranes where other materials are embedded in a polymer matrix. One of the most common and commercially available PEM materials is Nafion, a DuPont product. While Nafion is an ionomer with a perfluorinated backbone like Teflon there are many other structural motifs used to make ionomers for proton exchange membranes. Many use polyaromatic polymers while others use partially fluorinated polymers.

Proton exchange membranes are primarily characterized by proton conductivity (σ), methanol permeability (P) and thermal stability.

1.3.3 Glass Electrolyte

The third class of electrolytes is the family of amorphous conductors. These conductors are more close to liquid electrolytes than crystalline ion conductors. Amorphous ion conducting materials have some unique properties such as isotropic properties, absence of grain boundaries, easy film formation and so on. A new porous glass electrolyte consisting of heteropolyacids (phosphotungstic acid (PWA) and phosphomolybdic acid) was investigated and was found to yield a remarkably high proton conductivity of 1.01 S cm^{-1} at 30 °C and 85% relative humidity. This is the first time reported such a high proton conductivity value for a heteropolyacid glass membrane. The glass was applied as the electrolyte for an H_2/O_2 fuel cell and a maximum power density of 41.5 mW/cm^2 at 32 °C was attained using this new PWA-containing electrode [3].

1.3.4 Fluorite-Structured Electrolytes

The fluorite structure is a face–centred cubic arrangement of cations with anions occupying all the tetrahedral sites, leading to a large number of octahedral interstitial voids as shown in Figure 1.1 Thus this structure is a rather open one and rapid ion diffusion might be expected. At high temperature, zirconia has the fluorite structure stabilised by addition of divalent or trivalent (aliovalent) cations such as Ca or Y at lower temperatures. Pure ceria also has the fluorite structure. Oxide ion conduction is provided by oxide ion vacancies and interstitial oxide ions. In the case of pure ZrO_2 and CeO_2, electrical conductivity is quite low because the concentration of the oxide ion vacancies and interstitial oxide ions is low. However, as dopants such as yttria are added, the conductivity increases. Each additional yttria molecule creates one oxygen vacancy. The concentration of the vacancies is given simply by the electrical neutrality condition.

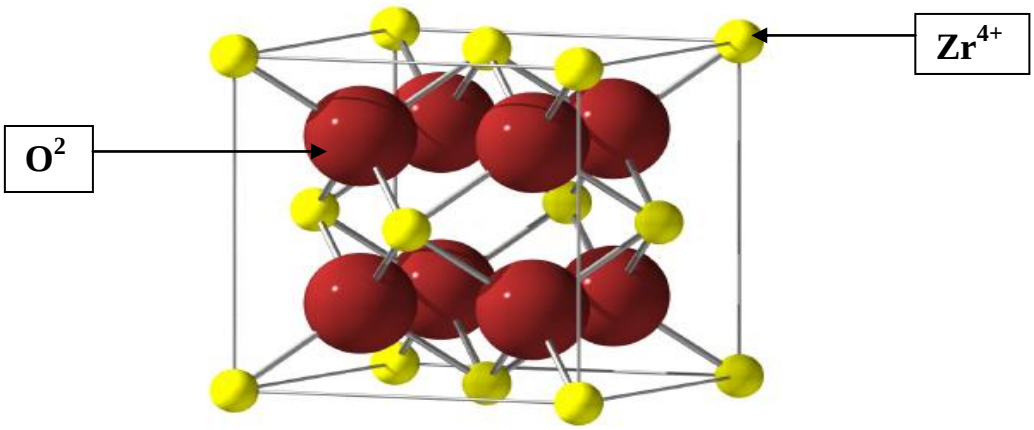

Figure 1.1 Fluorite structure of ZrO_2.

1.3.5 Perovskite-Structured Electrolyte

In addition to fluorite structure electrolyte such as stabilised zirconia and ceria there are many non-fluorite structure oxide which are potentially attractive for SOFC electrolyte application. These include perovskite like lanthanum gallate ($LaGaO_3$) and to a lesser degree calcium titanate ($CaTiO_3$) as shown in Figure 1.2 The perovskite based on the general formula ABO_3 comprise a rich family of compounds with important

applications such as solid oxide fuel cell, ferroelectric, superconducting materials and oxidation catalysts.

Due to high stability of the crystal structure and the variety of cations which can be accommodated within it perovskite display a variety of properties. Many display both ionic and electronic conductivity and so are useful as electrodes in SOFCs. Only few perovskite are purely ionic in their conduction behaviour.

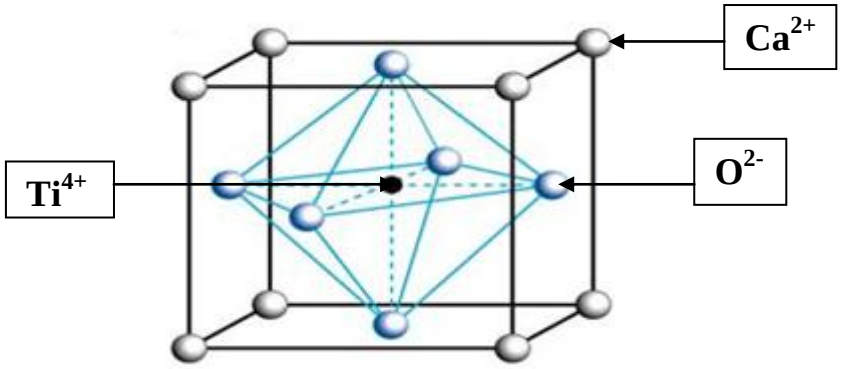

Figure 1.2 Perovskite structure of $CaTiO_3$.

1.3.6 Pyrochlore-Structured Electrolyte

Pyrochlore oxides are named after the mineral pyrochlore, $(NaCa)(NbTa)O_6F/(OH)$, with which they share a similar structure. $A_2B_2O_7$ pyrochlores are ternary metallic oxide whose crystal chemistry is complex enough to make them favourable for a wide range of applications. Here A and B cations are considered as having charge of 3^+ and 4^+ respectively. However, there is another entire series of pyrochlore compounds consisting of 2^+ and 5^+ cations.

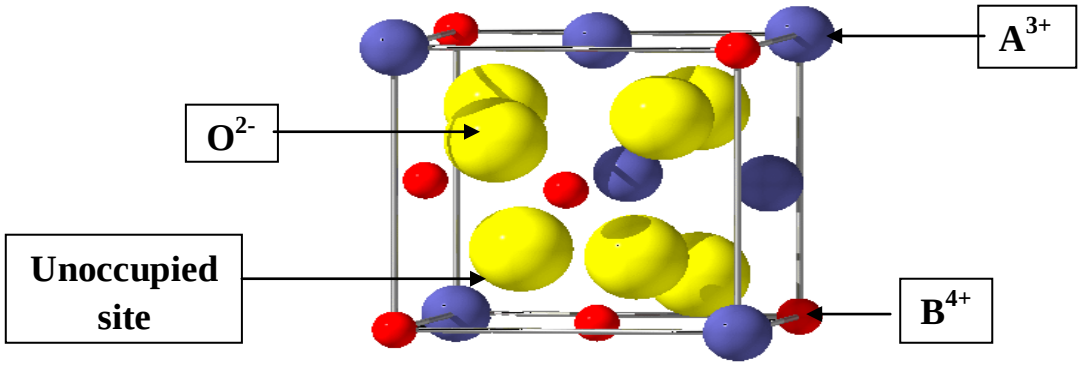

Figure 1.3 Unit cell of pyrochlore.

The more general crystal structure describes materials of the type $A_2B_2O_6$ and $A_2B_2O_7$ where the A and B species are generally rare-earth or transition metal species; e.g. $Y_2Ti_2O_7$.The pyrochlore structure is a super structure derivative of the simple fluorite structure (AO_2 = A_4O_8, where the A and B cations are ordered along the <110> direction. The additional anion vacancy resides in the tetrahedral interstices between adjacent B-site cations.

In this description of pyrochlore, the A and B cations form the face centred cubic array, but are additionally ordered in the <110> directions such that the A cations are eight coordinate and the B cations are six coordinate with respect to oxygen. This cation ordering means that the tetrahedral anion sites are no longer crystallographically identical. Figure 1.3 depicts one eighth of the pyrochlore unit cell, which is analogous to a single fluorite unit cell.

1.4 Characteristics of Solid Electrolyte

Good electrolyte is supposed to have crystal structures with open channels, layers so as to provide pathways for easy ionic transport via hopping mechanism. High conducting electrolytes are required to fulfill the following conditions:

a) Availability of large number of free ions for good ionic conduction (should be characterized by oxygen ion transport numbers close to unity)

b) Large number of vacancies for hopping

c) Same energies of the occupied and vacant sites

d) High polarizability of the anion framework

e) Electronically insulating

f) Chemically stable at high temperature as well as in reducing and oxidizing conditions

g) Gas tight/free of porosity

h) Uniformly thin layer (to minimize ohmic losses)

i) Thermal expansion coefficient should match with electrodes of SOFC

j) Use inexpensive materials

1.5 Materials for Solid Electrolyte

Materials research is being conducted around the world with many different material sets under consideration and with several approaches for development and use of such in fuel cells. Much of this research and development is driven by the need for cost reduction. The cost reduction in general can be accomplished by: increasing power density (enhancing the performance characteristics of fuel cell electrolyte), lowering operating temperature (reducing the cost of materials of construction) and enhancing manufacturability (eliminating or reducing the cost of manufacturing steps).

High ionic conductivity of the solid electrolyte can be achieved by optimization in the structure. Some materials exhibit higher ionic conductivity but they are very expensive, for example Yb_2O_3 [4]. These materials find limited applications due to cost factor. The mostly investigated materials are the fcc fluorite–type oxide ion conductors based ZrO_2, CeO_2, and Bi_2O_3. Doped ZrO_2, CeO_2 and Bi_2O_3 are considered as ideal electrolyte materials for ceramic oxygen generators and solid oxide fuel cell (SOFC).

Among these, the electrolyte materials derived from bismuth oxide (Bi_2O_3) compositions show the highest conductivity as compared to others, particularly below 600 ^oC. Takahashi and Iwahara [5] were the first to attempt the stabilistion of the fluorite-type phase to room temperature of Bi_2O_3 in the early 1970. Nearly 30 years later cubic bismuth oxide remains the highest conducting solid oxide electrolyte due to both extremely high intrinsic oxygen vacancy concentration and high anion mobility. The high mobility is due to weak Bi-O bond and the high polarizability of Bi^{3+} with its lone pair of $6s^2$ electrons. The high intrinsic concentration of oxygen vacancies is a result of obtaining the fluorite structure with a Bi^{3+}. At about 600 ºC all of the cubic phase stabilised bismuth oxide exhibit a change in conductivity activation energy with a lower activation energy above ~600 ºC and a higher activation energy below ~600 ºC [6].

Unlike ZrO_2 and CeO_2 in which divalent or trivalent dopant cations must be added in order to introduce the oxide ion vacancies critical for ionic conductivity, the fluorite-type form of Bi_2O_3, δ-Bi_2O_3 has intrinsic vacancies. In fact 25% of the oxide ion sites are vacant in this material.

Generally yttria-stabilised zirconia (YSZ) is used as solid electrolyte material for SOFC. However, SOFC containing YSZ must be operated above 950ºC in order to achieve sufficient power density. Now a days, most of the research have been carried out on these materials to develop highly oxide ion conductive solid electrolyte at lower operating temperature.

Bismuth oxide (Bi_2O_3) has recently been studied for possible application in SOFC (solid oxide fuel cell). It was found that it is much better than YSZ in terms of oxygen ionic conductivity. Doped bismuth oxide exhibit superior ionic conductivity over YSZ and CeO_2 based electrolytes at lower temperature. δ-Bi_2O_3 is recognized as one of the most technologically important oxide ion conductors because it can be used as the solid electrolyte material in fuel cells, high temperature oxygen pumps and many different sensors. The δ-phase is one of the four known polytypes of Bi_2O_3 solid, and it is stable only in the temperature range from 730 °C to its melting temperature of 825 °C. δ-Bi_2O_3 has high ionic conductivity at 750 ºC of ~1 Scm^{-1} and is the most highly conductive oxide ion conductor known [7].

1.5.1 Polymorphism of Bi_2O_3

As mentioned above Bi_2O_3-based solid electrolyte materials with fcc fluorite-type structure are of interest due to their high oxide ion conductivity. However, δ-Bi_2O_3 is stable only between 730 ºC and its melting point of 825 ºC [7]. Pure Bi_2O_3 has a monoclinic structure at room temperature, which transform to δ-Bi_2O_3 when heated above 730 ºC. The behaviour of Bi_2O_3 on cooling from the δ-phase is more complex and depends on the sample thermal treatment, with the possible trasformation of the intermediate, metastable, tetragonal β-phase at ~650 ºC, which transform to α-Bi_2O_3 at 300 ºC. The bcc γ-phase can form at ~640 ºC, and can be preserved to room tempertaure with very slow cooling rate. Two other metastable polymorphs, the orthorhombic ε-Bi_2O_3 and triclinic ω-Bi_2O_3 have also been reported [8]

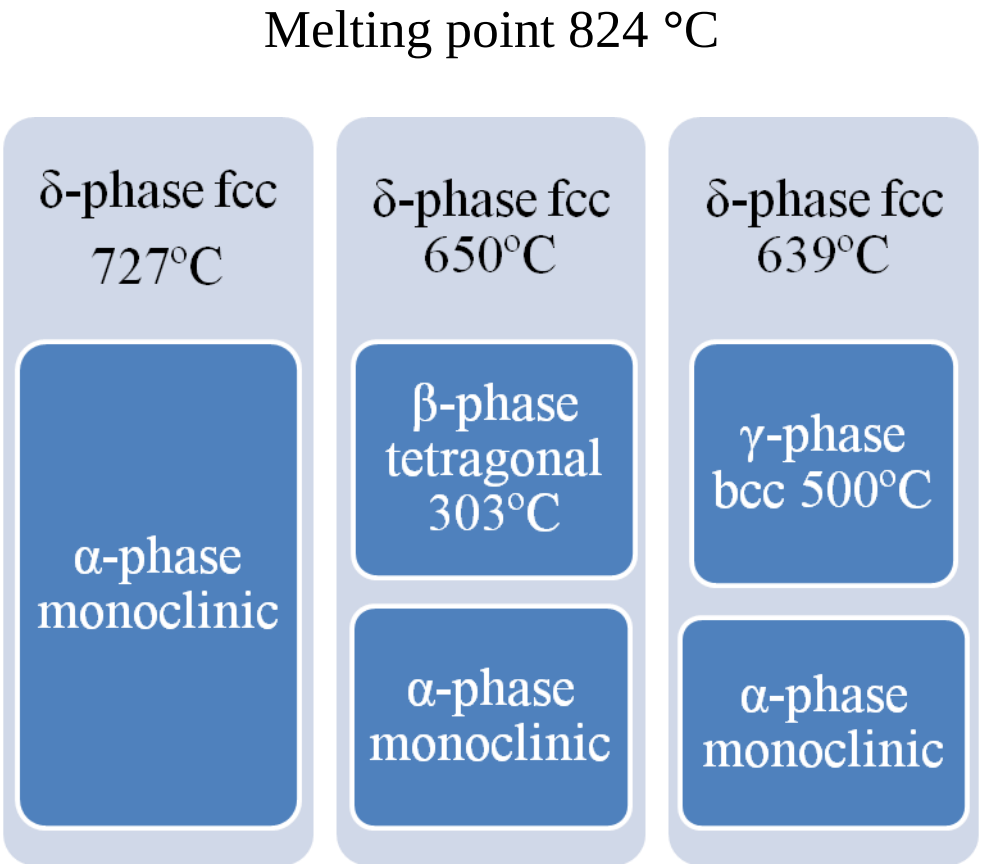

Figure 1.4 Existing domains of the four polymorphs of Bi_2O_3 as a function of temperature.

Harwig and Geraards [9] systematically measured the conductivity of α, β, γ and δ-Bi_2O_3, and found that the conductivity of δ-Bi_2O_3 was predominately ionic, about three orders of magnitude greater than β and γ phases, and about four orders of magnitude greater than α-phase. In addition to electrical properties, thermal expansion properties are very important when considering for solid electrolytes. High thermal expansion coefficients represent large dimensional variations during heating and cooling which would limit the performance of a solid electrolyte. The transition from the high-tempertaure δ-Bi_2O_3 to the intermediate β-Bi_2O_3 is accompanied by a large volume change and as a result of deterioration of the mechanical properties of the materials. It is therefore necessary to stabilise δ-Bi_2O_3 to room temperature to avoid problems associated with phase transitions, before it is suitable for practical use as solid electrolyte.

However, δ-Bi_2O_3 can be stabilized by dopants which include rare-earth elements and many oxide impurities (from divalent to hexavalent oxides). The ionic conductivity of pure δ-Bi_2O_3 is known to arise from the oxygen vacancies and the concentration of such vacancies can be as high as 25% of the total amount of anions. With such a high concentration of oxygen vacancies the conductivity of δ-Bi_2O_3 can be two orders of magnitude higher than that of the common oxide conductor zirconia [10].

In addition, the conductivity can be further raised by the incorporation of appropriate dopants, particularly rare-earth dopants, into δ-Bi_2O_3 [11]. The conductivity of various phases of Bi_2O_3 is given in Table I.

Table I Conductivity of the various phases of Bi_2O_3 [12]

Phase	**Conductivity at 600 °C (Scm^{-1})**	**Conductivity at 650 °C (Scm^{-1})**
α-Bi_2O_3	~10^{-4}	3×10^{-4}
β-Bi_2O_3	~10^{-4}	2×10^{-3}
γ-Bi_2O_3	~3×10^{-3}	5×10^{-3}
δ-Bi_2O_3	-	1

1.5.2 Structure of δ-Bi_2O_3

The high conductivity of δ-Bi_2O_3 can be attributed firstly to high polarisability of the Bi^{3+} cations, with its $6s^2$ lone pair of electrons [13]. Smart and Moore [14] define the polarisibilty of an ion as the ease of distortion of its electron cloud, making the passage of a mobile ion (oxide ion) through the Bi^{3+} sublattice easily. The lone pair usually occupies a volume of the same order of magnitude as that of oxide ion [15].

Generally, doping induces the increase of oxygen vacancies. For trivalent Y or rare-earth metal, the compensation of charges does not exist at substitution. The oxygen vacancies mainly results because of the formation of lone pair electron in Bi atom or crystal distortion.

Bi_2O_3–based materials decompose to metallic bismuth when exposed to reducing SOFC gases such as hydrogen or methane, but this problem might be reduced by using a bilayer electrolyte where the Bi_2O_3–based materials is protected from the reducing gases

by a thin layer of YSZ [16]. Since, δ-Bi_2O_3 is structurally stable only between 730 ºC and its melting point of 825 ºC and cannot be quenched to room temperature. However, there has been much research focus on finding doped Bi_2O_3-based materials for which the fluorite–type trying to preserve the high conductivity and improve the long term stability of the structure and conductivity.

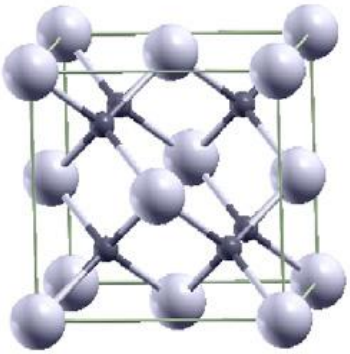

Figure 1.5 Unit cell for δ-Bi_2O_3. Big spheres and small spheres are Bi and O atoms, respectively.

1.5.3 Doped Bi_2O_3-based materials

Indeed, Bi_2O_3 easily forms solid solutions with many other metal oxides. These doped system exhibit a complex array of structure and properties dependent on the type of dopant, the dopant concentration and the thermal history of the sample. The structures and properties of both δ-Bi_2O_3 and Bi_2O_3 doped system have been characterised using a number of technique. The addition of rare-earth cations with large ionic radii, such as La^{3+} and Nd^{3+} to Bi_2O_3, typically produces rhombohedral layered solid solution phases at room temperature after air quenching, rather than fluorite-type materials [15]. The fluorite-type phase can be preserved to room temperature, by the adddition of smaller rare earth cations from Sm^{3+} to Lu^{3+} including Y^{3+} [17]. The expressions "preserved to room temperature"are appropriate to describe the known room temperature fluorite-type materials rather than "stabilised" because the fluorite-type materials are metastable and undergo transformations during long term heat treatment at intermediate temperature (~500 ºC to 650 ºC). Many researches have been tried different dopant to achieve high ionic conduvtivity in intermediate temperature range [18-20]. Titanium doped bismuth might be shown good ionic conductivity. Therefore, in the present study, the titanium doped bismuth is chosen to study the effect of dopant on various properties of bismuth

1.5.4 Phase-diagram of Bi_2O_3-TiO_2 system

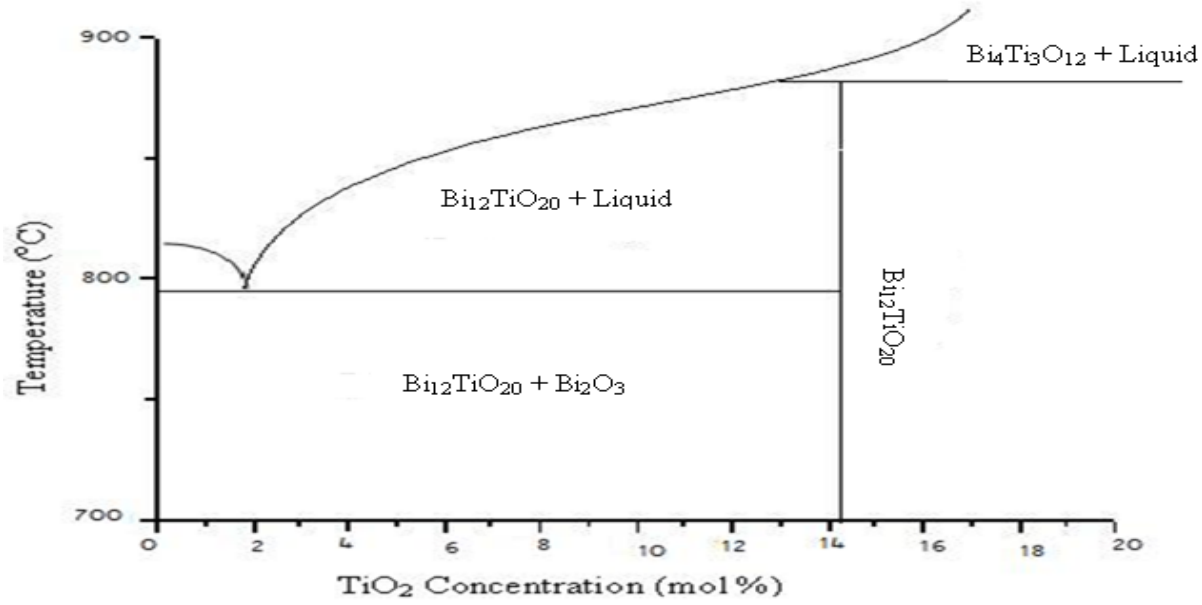

Figure 1.6 Phase diagram of Bi_2O_3-TiO_2 system [21].

Figure 1.6 shows the substantial phase diagram drawn by the experimental results described above. The eutectic and the peritectic temperatures were determined to be 823 ºC and 855 ºC, Hereafter, we focus on a TiO_2-poorer region than the stoichiometric $Bi_{12}TiO_{20}$ (BTO), because the single crystals are grown only from hypo-peritectic solutions. The phase diagram shown in Figure 1.6 starting solutions with a TiO_2 concentration of lower than the peritectic composition (～12 mol %) provides the BTO single phase. Polycrystalline phases consisting of Bi_2O_3, BTO and $Bi_4Ti_3O_{12}$ were obtained from 11.00 and 11.25 mol % TiO_2 solutions, while single phase BTO crystals were obtained from 10.25 and 10.50 mol % TiO_2 solutions. After 10.75 mol % TiO_2 solutions indicated first crystallied part was the lamellae-type $Bi_4Ti_3O_{12}$ phase and the BTO single phase crystallization after the while resulted from a gradual change in solution composition passing the peritectic composition along the liquidus curve. Therefore, we emphasize that the substantial peritectic composition must lie close to a 10.75 mol% TiO_2 concentration or less to some degree.

1.5.5 Effect of ionic polarizability in δ-Bi_2O_3

Cubic bismuth oxide (δ-Bi_2O_3) is a fluorite-based material and has one of the highest oxygen conductivities making it a good electrolyte material for solid oxide fuel cells (SOFCs). This high conductivity phase is stable only over the very narrow temperature range from 730 ºC to 825 °C. δ-Bi_2O_3 can be stabilized to lower temperature by doping with aliovalent dopants. As this doping can stabilize the fluorite phase to lower temperature, the resulting solid solutions undergo a rapid decrease in conductivity due to ordering of the oxygen sublattice [22]. The oxygen sublattice ordering originates from the rearrangement of the two structural oxygen vacancies present in the fluorite-type unit cell of δ-Bi_2O_3. The high conductivity of pure δ-Bi_2O_3 is due to the high polarizability of its $6s^2$ lone pair of electrons [13]. When both the Bi and O ion polarizabilities are assigned their maximum values, the system represents real δ-Bi_2O_3. In the polarizabilities of the ions, it is found that the bismuth ions vibrate around their respective lattice sites and do not diffuse. So, the mobility of the oxygen ions depends strongly on their polarization. When the ions are non-polarizable, there is some initial (<150 ps) oxygen motion; after this time, oxygen diffusion ceases completely the resulting structure consists of a vacancy-ordered structure that does not allow further diffusion [23]. In contrast to the vacancy ordering in non-polarizable system, the fully-polarizable system allows continuous oxygen diffusion.

The system in which both the Bi and O are fully polarizable the system represents real δ-Bi_2O_3. A critical Bi polarizability (>2.5$Å^3$) is required for continuous diffusion to take place, thereby preventing the formation of the vacancy-ordered structure that suppresses the ionic conduction [6, 24]. When the Bi ions are polarizable, one can imagine that the diffusion of a negatively charged oxygen ion will be facilitated by charge separation, with the negatively charged electronic lone pair of Bi ions being displaced from the oxygen ion and the positively charged ion core being displaced closer to the oxygen ion. This separation of charge should result in a stronger Coulombic interaction of the O ion to the Bi ion, thereby lowering the energy barrier to diffusion of oxygen between two Bi ions.

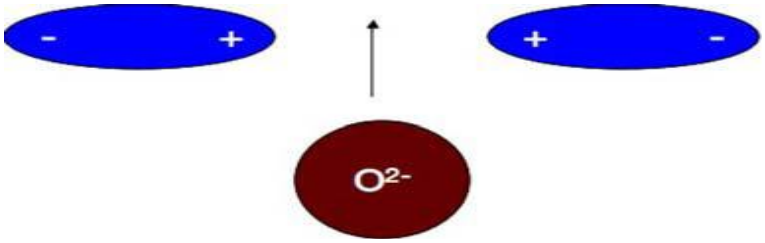

Figure 1.7 Oxygen ion diffusion through two Bi ions.

1.5.6 Ionic conduction of δ-Bi_2O_3

Much research has been aimed at finding materials that best preserve the high conductivity of pure δ-Bi_2O_3. In the nonempirical calculations carried out on the basis of the Sillen model, two oxygen vacancies were arranged along crystallographic axes {111}. In the Willis model, six oxygen atoms were randomly distributed over 8c site and each 8c site surrounded by four 32f sites. Each 32f site is at a distance of 0.48 Å in <111> from 8c [6, 24].

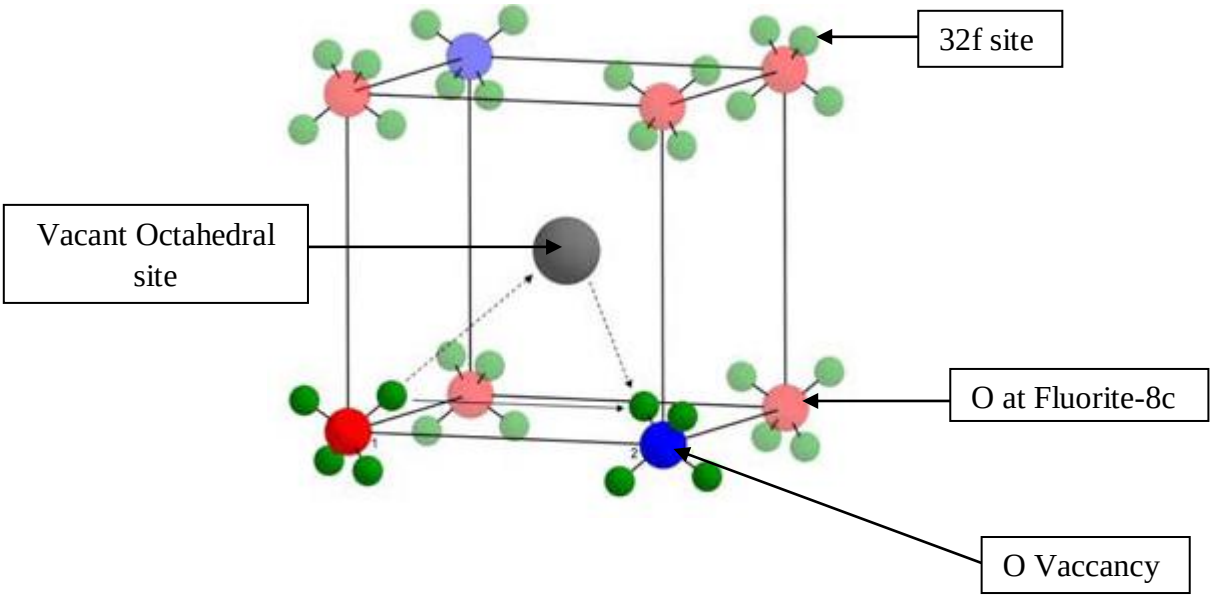

Figure 1.8 A cubic oxygen sublattice in a fluorite crystal structure.

An oxygen atom diffuses to a vacant site via 32f sites. The conduction band of Bi is of the metallic type and is formed mainly by the p states. The valence band of bismuth oxide is filled completely. The high ionic conductivity of these phases is determined by the presence of a large number of vacant positions with low potential barriers for migration. Along with the analysis of the electronic structure of cubic bismuth oxide,

we analyzed the chemical bond for the δ-Bi_2O_3, α-Bi_2O_3, and β-Bi_2O_3 phases. The estimates of average overlap population of Bi–Bi and Bi–O bonds according to Mulliken are presented in Table II [25]. The interaction in the phases of bismuth oxide mainly occurs due to the covalent Bi–O bonds. The average occupancy of the Bi–O bond in the series α-Bi_2O_3, β-Bi_2O_3, and δ-Bi_2O_3 gradually decreases and has a minimum value for the fluorite-like structure of bismuth oxide. The minimum overlap population of the Bi–O bond in δ-Bi_2O_3 corresponds to oxygen mobility in the structure of the cubic bismuth oxide, i.e., to a high ionic conductivity. The covalent component of the Bi– Bi bond in all modifications of bismuth oxides is virtually equal to zero. Results of the analysis of the chemical bond were used for studying the possible models of conduction in cubic bismuth oxide. The presence of a sufficient number of vacant positions in the crystal structure and the low potential barrier to migration of the mobile ion are the chief factors determining the conductivity of ionic and superionic conductors.

In the fluorite-like structure δ-Bi_2O_3, two mechanisms of migration of oxygen ions are possible in accordance with the Willis model: through the centers of the Bi_4 tetrahedral and of the Bi_6 octahedral or bypassing octahedral interstices [25, 26]. The preferability of either of the mechanisms was estimated from the difference in the total energies of a perfect crystal and a crystal with an oxygen atom shifted to octahedral or tetrahedral interstices. The results of analysis proved that the total energy of the crystal changes by 0.7 eV when an oxygen atom is shifted to a tetrahedral interstice and by 3.2 eV in the case of an octahedral interstice [27]. We can assume that the migration of oxygen ions takes place through tetrahedral voids in the fluorite structure rather than through octahedral positions.

Table II Average bond population by Mulliken for α-Bi_2O_3, β-Bi_2O_3, and δ-Bi_2O_3 [25]

Phase	**Bond population**	
	Bi-O	**Bi-Bi**
α-Bi_2O_3	0.15	0.05
β-Bi_2O_3	0.14	0.01
δ-Bi_2O_3	0.07	0.00

1.6 Ionic conductivity and solid electrolyte

High ionic conductivity in crystalline solid materials is widely recognised; although still is relatively rare, phenomenon. Most ionic solid are electrical insulators unless they exhibit electronic conductivity. They begin to show significant level of ionic conductivity only at higher temperatures as the melting point is approached. Materials in the family of crystalline solid electrolyte exhibit high ionic conductivity in one of their sublattices – *the mobile ion sublattices*- at temperature well below melting point and often as low as room temperature. Four classes of solid ionic conductors may be distinguished

- Ion exchangers which are solids capable of exchanging some of the ions that participate in their structure. This means a high mobility of the two exchanging species at ambient (operating) temperatures.
- Electrolytes which are ideally electronic insulators and excellent conductors of a single ionic species selected for a specific application
- Electrodes
- Chemical stores

Each has important applications with different fabrication requirements. Fast ion transport is required in electric power applications, and various strategies are discussed for power batteries. The design of new materials begins with a theoretical model for ionic transport; the situation in stoichiometric compounds is compared with that in doped compounds, and electrolytes are contrasted with mixed ionic – electronics.

In solid-state ionic, fast ion conductors, also known as solid electrolytes and superionic conductors, are materials that act as solid state electrical conductors and are used primarily in solid oxide fuel cells. As solid electrolytes they conduct due to the movement of ions through voids, or empty crystallographic positions, in their crystal lattice structure having high ionic conductivity and minimal electronic conductivity comprising a stable wide energy gap between the bond band and the conduction band. The most commonly used solid electrolyte is yttria-stabilized zirconia, YSZ. One component of the structure, the cationic or anionic, is essentially free to move throughout the structure, acting as charge carrier. Fast ion conductors are intermediate

in nature between crystalline solids which possess a regular structure with immobile ions, and liquid electrolytes which have no regular structure and entirely mobile ions.

Ionic conductivity is important for many products:

- Type I and type II batteries (i.e. regular and rechargeable).
- Fuel cells.
- Electrochromic windows and displays.
- Solid state sensors, especially for reactive gases.

In contrast to purely electronic current transport, there is always a chemical reaction tied to the current flow that takes place wherever the ionic current is converted to an electronic current - i.e. at the contacts or electrodes. There may be, however, a measurable potential difference without current flow in ionic systems, and therefore applications not involving chemical reactions. This is a big difference to current flow with electrons (or holes), where no chemical reaction is needed for current flow across contacts since "chemical reactions" simply means that the system changes with time.

If we look at the conductivity of solid ionic conductors, we look at the movement of ions in the crystal lattice - e.g. the movement (= diffusion) of O^- or H^+ ions either as interstitials or as lattice ions. In other words, we look at the diffusion of (ionized) atoms in some crystal lattice, described by a diffusion coefficient D which is correlated to mobility μ - by the Einstein-Smoluchowski relation

$$\mu = \frac{e * D}{kT} \qquad (1)$$

1.6.1 Conduction Mechanism

Ionic conductivity occurs by means of ions hopping from site to site through a crystal structure therefore it is necessary to have partial occupancy of energetically equivalent or near equivalent sites. Two broad classes of conduction mechanism- vacancy and interstitial migration may be distinguished.

In vacancy migration a number of sites that would be occupied in the ideal, defect free structure are in fact empty perhaps due to either thermally generated Schottky defect

formation or the presences of charged impurities. An ion adjacent to vacancy may be able to hop into it leaving its own site vacant. This process is regarded as vacancy migration and not the vacancies that hop.

Interstitial sites are defined as those that would usually be empty in an ideal structure occasionally in real structure ions may be displaced from their lattices sites into interstitial sites (Frenkel defect). Once this happens the ions in interstitial site can often hop into adjacent interstitial sites. These hops may be one stage in a long range conduction process.

These two mechanisms may be regarded as isolated ion hops. Sometimes it is observed, especially, in solid electrolytes, cooperative ion migration occurs.

In crystalline electrolytes, conduction pathways for the mobile ions permeate the immobile ion sublattice in one, two and three dimensions depending on the structure of the materials. The site containing mobile ions are not fully occupied and are connected via open windows to adjacent sites that are also partially occupied or empty. Ionic conduction occurs, therefore by means of series of definite hops between adjacent sites in the conduction pathways. For most of the time, the mobile ions are located in a particular site where they undergo thermal vibration within the site. Just occasionally, they escape from their site and hop quickely into an adjacent site where they may then reside for a considerable time before either moving on or hopping back into original site.

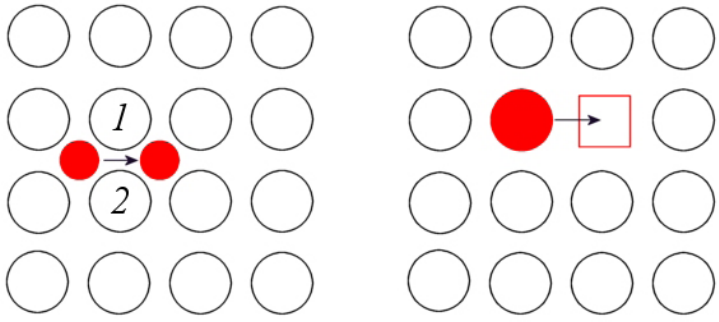

Figure 1.9 Interstitial and vacancy diffusion mechanisms.

Due to the severe lattice distortions required, larger atoms occupying interstitial sites are unable to diffuse via an interstitial mechanism. However, an alternative is afforded by

the interstitialcy mechanism, in which an interstitial atom forces an adjacent atom on a regular lattice site into an interstitial site

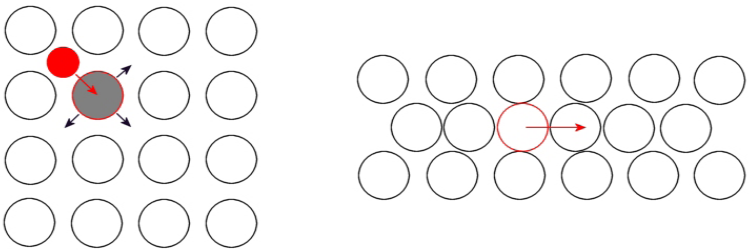

Figure 1.10 Interstitialcy and crowdion diffusion mechanisms.

This type of diffusion can be collinear (if the displaced atom moves in the direction arrow in above Figure) or non-collinear (if it moves in other directions than the red arrow). A related diffusion mechanism occurs when an interstitial occurs in a close packed direction, and is known as the crowdion mechanism. The extra atom in the row displaces several atoms from their regular sites. Although this mechanism is not likely for ionic materials because of the strong Coulombic forces involved, it may be important after irradiation, especially in metals. It has already been stated that it is not unlikely for several types of defects to be present simultaneously. Each of the diffusion mechanisms discussed is dependent on point defects. Therefore, several types of diffusion mechanism can co-exist, with one generally predominating. It follows that diffusion is directly related to the concentration of defects and their mobility.

1.7 Applications of Solid Electrolyte

Fuel Cell

As the requirements for cheap clean electrical energy source are increasing so fuel cells are becoming a viable source of power for many applications. Fuel cell offers a clean and pollution free technology for electricity generation. Stabilized zirconia is used as a solid electrolyte in fuel cells. At present several types of fuel cells are available in the consumer market and the following five types of fuel cells are commonly employed:

- Solid polymer proton conductor fuel cell (SPFC)
- Alkaline fuel cell (AFC)
- Phosphoric acid fuel cell (PAFC)

- Molten carbonate fuel cell (MCFC)
- Solid oxide fuel cell (SOFC)

Solid Fluoride Electrolytes in Chemical Sensors

Due to the combination of good ionic conductivity with low electronic conductivity, a number of solid metal fluorides are excellent electrolytes and thus have been used in chemical sensors for numerous applications ranging from room temperature oxygen gas sensors to sensors for use in the processing of molten metals. The most studied metal fluorides are those which form the cubic fluorite crystal structure, such as CaF_2, PbF_2, LaF_3 and MgF_2 have promising applications in chemical sensors.

Resistance Heating Elements

Doped zirconia is one of the few materials that can be operated as a resistance heating element at temperatures greater than 1800 °C in an oxidizing environment. For this application the conductivity of the ZrO_2 does not have to be purely ionic but can be a combination of ions and electrons.

Galvanic Cells for Thermodynamic and Kinetic Measurements

Solid electrolyte materials like doped zirconia solid electrolyte have been extensively for obtaining thermodynamic and kinetic measurements for metals, alloys, inter metallics, and oxide. Galvanic cells have been constructed for the measurements of standard free energy of formation of oxides and inter metallics, chemical activities in molten and solid metals and alloys, and diffusivity of oxygen in molten and solid metals.

Gas Sensors

Electrochemical cells containing solid electrolytes may be used for the measurement of partial pressures of gases or the concentration of gases dissolved in liquids. The most obvious type of sensor is a tube of yttria stabilised zirconia (YSZ) or other solid electrolyte.

Memory Devices

The need for embedded non-volatile memories has never been greater. System-on-chip (SoC) designs frequently require a non-volatile memory module which has a small footprint, low power, high endurance, high speed, and minimum additional process steps to reduce manufacturing complexity and cost. Emerging memories based on solid electrolytes offer an intriguing solution to the growing problem of inefficient non-volatile embedded memories. One such memory element is the programmable metallization cell (PMC), also known as conductive bridging random access memory (CBRAM). To illustrate these benefits in the context of a memory array, the design of a 2-kb non-volatile memory block using solid electrolyte cells formed by sandwiching a Ag-Ge-Se electrolyte layer between individually addressable tungsten plugs and a silver common electrode.

Batteries

The solid electrolyte is a material with a high ionic conductivity and negligible electronic mobility. The application of solid electrolyte is in electrochemical device like battery in implantable electronics instrumentation such as cardiac pacemakers, physiological monitoring/telemetry package etc. Because of good electrode/electrolyte interface, high ionic conductivity, electrochemical stability, thermal stability, and mechanical strength. Solid electrolyte has better reliability, safety, flexibility, and processibility. Mohri *et al.* [28] have first reported Ni/MH –related batteries using Sb_2O_5 . xH_2O as a solid electrolyte.

Chapter 2

Literature Review

A solid electrolyte, for its application in SOFC, must fulfil certain criteria apart from the high oxygen-ion conductivity. It must be stable with respect to other cell components, have adequate thermal and mechanical properties, structural and thermodynamic stability in both reducing and oxidizing environments. In additions to this, it should have,- matching thermal expansion coefficient with other cell components and ionic transport number should be close to unity. If the ionic transport number is less than 1.0 then there are direct thermodynamic efficiency losses at least proportional to the electronic transport component. The cost of raw materials, the ease and economics of fabrication into desired shapes and sizes are some of the other equally important criteria.

There are generally four types of systems under consideration which are zirconia (ZrO_2), ceria (CeO_2), lanthanum gallate ($LaGaO_3$) and bismuth oxide (Bi_2O_3). Zirconia-based systems are the most stable with respect to fuel cell operating environments followed by lanthanum gallate, ceria - and bismuth oxide–based systems. These systems may be used in isolation or as a combination of two, for example, bi-layer structures consisting of a thin layer of doped zirconia on ceria - or bismuth oxide - based electrolytes for increased stability in reducing environments. With respect to other cell components both zirconia and ceria electrolytes are relatively inert, whereas doped bismuth oxides are reactive and their stability over the operating life of a commercial fuel cell stack is of serious concern. Other systems such as doped - thoria (ThO_2), doped -hafnia (HfO_2) offer no significant advantages over zirconia - based systems in terms of higher conductivity, better stability in fuel cell operating environments or stability.

2.1 Bismuth - based Systems

Bi_2O_3 exists in the monoclinic form at room temperature and is predominantly an electronic conductor. The high temperature (> 730 ºC) oxygen - ion conducting face centred cubic phase (or δ-phase) can be stabilised with the addition of a number of other metal oxides such as Y_2O_3, Dy_2O_3, Er_2O_3, Gd_2O_3, Nb_2O_5 and Ta_2O_5. For rare-earth doped materials, the minimum amount of the oxide phase required to stabilise the δ-phase at lower temperatures varies with the ionic radius of the stabilising cation [29].

Takahashi *et al.* [11] have shown that the stabilised cubic phase had the highest ionic conductivity amongst all oxygen-ion conductors.

Amarilla *et al.* [30] synthesized series of Bi_2O_3-based oxide $Bi_{2-x}U_xLa_xO_{(3+3x/2)}$ by two diferent methods and observed, on the basis of X-ray data that crystallize with cubic or hexagonal symmetry depending on the composition and synthesis procedure. In particular, the stabilisation of the fluorite-type structure as a single phase at room temperature has been achieved in the compositional range $0.154 \geq x \geq 0.091$. The annealing of materials at 600 ºC for 500h yields in all case a 'tetragonal' phase that is isolated as the only phase for x = 0.222

Since the main objective in the development of new materials for these application is to obtain electrolytes with higher conductivities and lower activation energies at lower temperature.

In recent years much attention was focused on materials known as BIMEVOX (BI: bismuth, ME: dopant metal, V: vanadium, OX: oxygen) related to a family of materials based on a narrow composition in the Bi_2O_3 - V_2O_5 system ($Bi_4V_2O_{11}$) where V is partially substituted by other cations such as Cu, Ti, Zn, Co, Mo and Ni and the discovery of fast oxide ion conductivity in $Bi_4V_2O_{11}$ [2]. Ionic conductivity of $4x10^{-4}$ Scm^{-1} has been reported by Yan and Greenblatt [31] for $Bi_4V_{1.70}Ti_{0.30}O_{10.85}$ at 223 ºC. Despite the high conductivity, they are reduced easily in atmospheres containing low oxygen partial pressures, have an extremely narrow electrolyte domain and are useful for limited electrochemical applications in the low temperature range (< 500 ºC). However, Chmielowiec *et al.* [32] presented a work concerns BIMEVOX based solid electrolyte doped with rare earth elements (lanthanum). Accroding to them, addition of

La_2O_3 increases the melting point and conductivity of $Bi_4V_2O_{11}$ by stabilization of high temperature good ionic conductive γ-$Bi_4V_2O_{11}$ phase upto 3% La content.

Kant *et al.* [33] have synthesized the Mn^{2+}-doped compounds $Bi_4V_{2-x}Mn_xO_{11-\delta}$ ($0 \leq x \leq 0.4$) by solid state reaction technique and investigated by X-ray diffraction and ionic conductivity measurement that high ionic conducting γ-phase is stabilized for $x \geq 0.2$. Whereas the ability to introduce Ga into V-site of $Bi_4V_{2-x}Me_xO_{11-\delta}$ leads to the stabilization of β-phase in the composition range $0.2 \leq x \leq 0.4$. The highest ionic conductivity is observed in $Bi4V_{1.8}Ga_{0.2}O_{11-\delta}$ with $\sigma = 3.40 \times 10^{-6}$ S/cm [34].

Krok *et al.* [35] have investigated the conductivity behaviour and cell parameter variation in the double substituted BIMEVOX system $Bi_2V_{0.9}Co_yCu_{0.1-y}O_{5.35}$. According to them, the volume of unit cell varies due to the microdomains of Co and Cu rich region in this double subsituted system. Also the low and high temperature conductivity increase with increase Co content, but overall conductivity appears to be lower due to the some type of defect trapping in the double substituted system.

Ekhelikar *et al.* [36] have synthesised solid solution of Y^{3+} and Gd^{3+} doped Bi_2O_3 and observed that solid solution containing 20-40 mol% of Y_2O_3 had fcc structure but Gd_2O_3 doped samples because of larger cationic radius of Gd^{3+} (0.94 Å) reveals that fcc phase is not stabilised and formed rhombohedral phase. So, fcc phase is stabilised by doping with oxides with relatively small cationic radius Y^{3+} (0.90 Å) than Bi^{3+} (1.03 Å).

Since pure or doped δ-Bi_2O_3 is the best high-temperature ionic conductor known. At the same time, when doped with stable and well known high conductivity of Zirconia several papers have been published regarding the Bi_2O_3-ZrO_2 system.

Abrahams *et al.* [37] concluded in the Bi_2O_3-ZrO_2 system, the formation of $Bi_{2-x}Zr_xO_{3+x/2}$ ($0.05 < x < 0.17$) occurs when the corresponding oxide mixture are quenched after heating at 850 ºC for 12 h. Substitution of Zr^{4+} for Bi^{3+} in the lattice results in the introduction of interstitial oxide ions. These oxide ions will contribute to total ionic conductivity. These β_{III}-phase which has a defect fluorite structure with ordered vacancies transform to show δ-Bi_2O_3 which has a fluorite structure with disordered vacancies on the oxygen sub-lattice [29].

The composition $Bi_{1.85}Zr_{0.15}O_{3.075}$ prepared by Abrahams *et al.* was further structurally characterized and refined in the tetragonal system. Since the structure of $Bi_{1.85}Zr_{0.15}O_{3.075}$ is similar to that of β-Bi_2O_3, the new phase was termed as β_{III}-phase.

Very recently, an increase of the Zr content up to x = 0.67 in the quenched $Bi_{2-x}Zr_xO_{3+\delta}$ with the β_{III}-Bi_2O_3 around 730 ºC and shows a segregation of a mixture of predominantly γ-Bi_2O_3 structure was reported again [38].

From the foregoing, it appears that there are considerable discrepancies regarding the compounds or solid solutions and their stability, particularly in the region with higher ZrO_2 contents.

Recently, the mechnochemical treatment of $2Bi_2O_3$-$3ZrO_2$ led to the gradual formation of very fine nanocrystalline phase, which resembled the high-temperature δ-Bi_2O_3. When mechnochemical treated samples were heated at 820 ºC. Now, slowly cooled, yield initial α-Bi_2O_3 and m-ZrO_2 phase rather than δ-Bi_2O_3 at room temperature as well as quenched sintered samples contained a mixture of β-Bi_2O_3 and m-ZrO_2 phase confirming that ZrO_2 stabilised β-Bi_2O_3 [39].

Sood *et al.* [40] synthesized a system (100-x)ZrO_2(x)Bi_2O_3 (x=5, 10, 15) in which a tetragonal $Bi_{7.38}Zr_{0.62}O_{12.31}$ phase has formed in all the samples after sintering at 850 °C for 24 h. Apart from this, ZrO_2 and Bi_2O_3 are also identified as minority phases. The volume fraction of $Bi_{7.38}Zr_{0.62}O_{12.31}$ phase increases with increasing concentration of Bi_2O_3.

Park *et al.* [41] designed bilayer SDC/ESB electrolyte .In this bilayer electrolyte SDC layer prevents the ESB layer from decomposing at very low P_{O2} and have a higher t_i transference number than single electrolyte layer. Also, the conductivity of this bilayer ESB/SDC is higher because of the formation of higher conductivity ESB phase in the SDC grain bondaries.

Zdujić *et al.* [42] synthesized nanocrystalline $Bi_{0.78}Hf_{0.59}Zr_{0.63}O_{3.61}$ solid solution with a fluorite-type δ-Bi_2O_3 structure by prolonged mechanochemical treatment of a powder mixture in a zirconia medium. The high value of electrical conductivity is, close to 0.1 Scm^{-1} make the mechnochemical synthesized solid solution a promising high oxide ion conductivity material.

Similarlly S.N. Ng *et al.* [43] synthesized materials Bi_2O_3-Nb_2O_5 binary systems successfully via a mechnochemical method at lower temprature than the solid state. Electrical measurements indicated that there was no significant difference in the conductivities synthesized by the two different methods.

As we know, the unit cell of the fluorite-type oxide consists of the so called M_4O_8 structure. The metal ion is suurounded by eight O-ion and O-ion is surrounded by four metal ions to form a tetragonal arrangement. The ratio of metal ionic radius to oxygen ionic radius should be greater than 0.732 in order to form a stable fluorite structure. Although the ratio of Bi ionic radius (1.17 Å) to oxygen ionic radius (1.38 Å) is 0.848, the high oxygen vacancy concentration still destabilizes the fluorite structure. In order to stabilize the fluorite structure, it is needed to reduce average cationic radius.

The sintered $(YO_{1.5})_{0.1}(WO_3)_{0.15}(BiO_{1.5})_{0.75}$ consists of a cubic fluorite structure and a very small amount of rhombohedral Y_6WO_{12}. The addition of Y_2O_3 reduces the mismatch in cation size and gives the average cationic radius of the matrix 1.06 Å [44].

Since, the ionic conductivity in Bi_2O_3 based materials depend on the mobility of anion in the fluorite structure as mentioned above. The high mobility is due to high polarizability of Bi^{3+}. So, the polarizability of the cations plays an important role in ionic conductivity. Also, all of the dopants typically used to stabilise the cubic structure of Bi_2O_3 are less polar than Bi^{3+}.

Polarizability is proportional to the cube of ionic radius [6]. The lanthanide dopants (Ln = Yb, Er, Ho, Dy) have both smaller ionic radii and lower polarizabilities than the host Bi ions. So, the conductivity in cubic bismuth oxide is reduced due to substitution of highly polarizable bismuth ions with less polarizable lanthanide ions in the cation sublattice. Dysprosium, which has the highest radius and highest polarizability among all dopants, exhibited the least decay in conductivity.

With the excellence in oxide ion conductivity of Bi_2O_3 based materials have turned out to be best for many application like separation of oxygen from air, SOFC, chemical sensor etc. A considerable number of studies have been done on the crystal structure, ionic conductivity of bismuth oxide based materials. However, the mechanical properties of the materials have been investigated in the application of devices by

Paydar *et al.* [45] According to them the addition of 3Y-TZP particles in BICUVOX enhance the mechanical properties by distributing the particles along grain boundaries of BICUVOX. These distributions reduce the grain size without degrading the ionic conductivity.

Table III provide the list of different electrolyte materials. Singhal and Kendall [46] note that stabilized zirconia and ceria possessing the fluorite structure has been the most favored SOFC electrolytes with perovskites, brownmillerites and hexagonal structured oxides as more recent alternatives. Among the candidate materials, zirconia is a relatively cheap base material and is by far the most popular electrolyte material for SOFC. Among the available electrolyte materials, operating temperature is very important to electrolyte performance.

Table III List of different electrolyte materials [47]

Systems	Acronym	Formula
Zirconia electrolytes	YSZ	$(ZrO_2)_{1-x}(Y_2O_3)_x$ (x~0.08–0.1)
	SSZ	$(ZrO_2)_x(Sc_2O_3)_{1-x}$ (x~0.8)
	CaSZ	$Zr_{0.85}Ca_{0.15}O_{1.85}$
Ceria electrolytes	GDC	$Ce_xGd_{1-x}O_y$ (x~0.8, y~1.8)
	SDC	$Ce_xSm_{1-x}O_y$ (x~0.8, y~1.9)
	YDC	$Ce_xY_{1-x}O_y$ (x~0.8, y~1.96)
	CDC	$Ce_xCa_{(1-x)}O_y$ (x~0.9, y~1.8)
Lanthanum electrolytes	LSGM	$La_xSr_{1-x}Ga_yMg_{1-y}O_3$ (x~0.9, y~0.8)
	LSGMC	$La_xSr_{1-x}Ga_yMg_{1-y-z}Co_zO_3$(x~0.8,y~0.8,z~0.085)
	LSGMF	$La_xSr_{1-x}Ga_yMg_{1-y-z}Fe_zO_3$ (x~0.8, y~0.5, z~0.4)
	LSGMCF	$La_{0.8}Sr_{0.2}Ga_{0.32}Mg_{0.08}Co_{0.2}Fe_{0.4}O_3$
	$LaAlO_3$ Based	$La_{1-x}Ca_xAlO_3$ (x = 0.0027–0.008)
		$La_{1-x}Ba_xAlO_3$ (x = 0.1)
Others	BCY	$BaCe_xY_{1-x}O_3$ (x~0.25)
	YSHa	$(HfO_2)_{1-x}(Y_2O_3)_x$ (x~0.08–0.1)
	YSTh	$(ThO_2)_{1-x}(Y_2O_3)_x$ (x~0.08–0.1)
Pyrochlorores-based		YZr_2O_7, $Gd_2Ti_2O_7$
Barium brownmillerites		$BaZrO_3$,$BaIn_2O_5$,$Ba_3Sc_2ZrO_8$
Strontium brownmillerites		$Sr_2ScAl_xA_yO_z$ (A=Mg, Zn), Sr_2ScAlO_5, $Sr_3In_2HfO_8$

Table IV presents approximate conductivities for selected electrolyte materials. Among the various materials listed below YSB and LSGMC provide the good conductivity in the temperature range 600 °C-800 °C. For 800 °C–1000 °C LSGMC and GDC provide the good conductivity.

Table IV Approximate conductivities (Scm^{-1}) for selected electrolyte materials [48]

Solid electrolyte		600 °C	700 °C	800 °C	900 °C	1000 °C
Zirconia electrolytes	YSZ	2.82E-03	8.29E-03	2.00E-02	4.13E-02	7.64E-02
	SSZ	2.51E-02	5.38E-02	1.00E-01	1.67E-01	2.58E-01
	CaSZ	1.78E-04	8.69E-04	3.16E-03	9.23E-03	2.28E-02
Ceria electrolytes	GDC	2.82E-02	7.30E-02	1.58E-01	3.01E-01	5.18E-01
	YDC	1.00E-02	2.01E-02	3.55E-02	5.68E-02	8.46E-02
	CDC	5.01E-03	1.30E-02	2.82E-02	5.36E-02	9.21E-02
Lanthanum electrolytes	LSGM	3.16E-02	7.69E-02	1.58E-01	2.89E-01	4.79E-01
	LSGMC	5.62E-02	1.20E-01	2.24E-01	3.74E-01	5.77E-01
Other electrolytes	YSB	1.00E-01	1.89E-01	3.16E-01	-	2.02E-01
	YsTh	5.62E-05	3.12E-04	1.26E-03	4.00E-03	1.06E-02

2.2 Aim of work

In all over the world, extensive research is going on to synthesize appropriate electrolyte material for solid oxide fuel cell application. Till date Y_2O_3 stabilized zirconia is most suitable electrolyte materials due to it has 0.1 S/cm ionic conductivity at 1000 ºC. Moreover, it shows good chemical and structural stability in oxidizing and reducing atmosphere. However, its ionic conductivity reduces drastically below 800 ºC. Therefore, to develop lower operating temperature (600 ºC-800 ºC) SOFC, some other electrolytes are being explored for their suitability as solid electrolytes. Bi_2O_3-based system shows better ionic conductivity below 800 ºC. However, ionic conductivity of this system can be increased by doping with isovalent and aliovalent cation. However, its melting point is 850 ºC with less phase stability. Moreover in long duration Bi^{3+} cations segregated along the grain boundary and affect the efficiency of cell. The stability of bismuth oxide can be enhanced by adding oxide impurity (divalent to hexavalent). According to Abraham et al. [37] by making solid solution of Zr for Bi in the host Bi_2O_3 results in the introduction of interstitial oxide ions which are responsible for conduction mechanism. $Bi_{1.85}Zr_{0.15}O_{3.075}$ system at 750 ºC, δ-phase having fluorite structure with vacancies in the oxygen sub-lattices [37]. The main objective of our study is to synthesize and investigate the TiO_2 doped bismuth-based solid electrolyte for lower temperature SOFCs application. So, In the present

study Ti doped $(Bi_2O_3)(1-x)(TiO_2)x$ $(0.05 \leq x \leq 0.2)$ systems will be synthesized by solid state reaction technique. These samples are named as BT1 (x=0.05), BT2 (x=0.10), BT3 (x=0.15) and BT4 (x=0.20) respectively. These prepared samples will be characterized by different techniques in chapter 3.

Chapter 3

Methodology and characterization

3.1 Sample Preparation

The composition $(Bi_2O_3)_{1-x}(TiO_2)_x$ for x = 0.05, 0.10, 0.15, 0.20 were prepared by using standard solid reaction technique. Sample label and their composition are given in Table V. Appropriate quantities of the rquired consitituent oxides of high purity fine powders were thoroughly mixed in acetone for 2 h, using mortar and pestle and dried by evaporation in air. This mixture was heated at 700 ºC for 4h in silica crucible and slowley cooled untill room temperature was reached. The calcination process was carried out in a pit furnace. The product thus obtained after heating was reground till a fine powder was obtained and cold pressed into pellets by adding binder (PVA), that were sintered from 800 ºC-820 ºC for 12 h depending on the composition and the melting point of the materials in order to obtain sintered pellets of density >90%. It was observed that the greater the content of doped oxide the higher was the sintering temperature. These entire samples were prepared in tublur frunace.

Table V Sample label with different composition

S.No.	Sample label	X
1.	BT1	0.05
2.	BT2	0.10
3.	BT3	0.15
4.	BT4	0.20

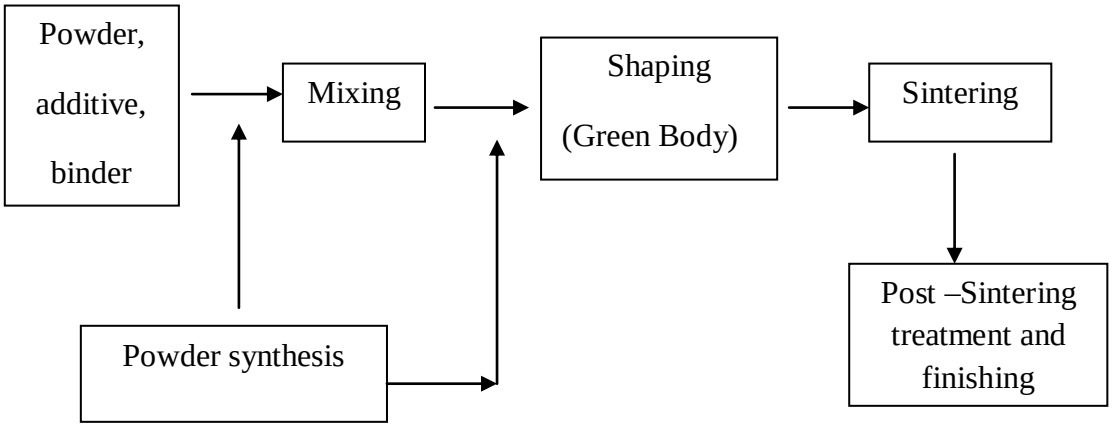

Figure 3.1: General processing patterns for sample preparation.

3.2 Characterization of materials

Characterization is an integral part of the study of any particular solid electrolyte. These include the understanding of polymorphism, structure determination, conductivity measurement and structure-conductivity relationship. For the analysis of above parameters, the samples were characterized using X-ray diffraction (XRD), differential thermal analysis (DTA)/thermal gravimetric analysis (TGA), scanning electron microscopy (SEM) and conductivity was measured by AC–impedance spectroscopy technique. The details of these techniques are given below:

3.2.1 X-Ray Diffraction

X-ray diffraction techniques are a family of non-destructive analytical techniques which reveal information about the crystallographic structure, chemical composition, and physical properties of materials and thin films. This technique is based on observing the scattered intensity of an X-ray beam hitting a sample as a function of incident and scattered angle, polarization, and wavelength or energy.

X-rays have wavelengths of the order of few angstroms (Å) the same as typical interatomic distances in crystalline solids. That means X-rays can be diffracted from materials which, by definition are crystalline and have regularly repeated atomic structures. When certain geometric requirements are met, X-rays scattered from a crystalline solid can constructively interfere, producing a diffracted beam. In 1912, W.

L. Bragg recognized a predicatable relationship among several factors. These factors are combined in Bragg's law as describe below:

$$2d \sin \theta = n \lambda \qquad (2)$$

where d = Interplanar spacing; λ = Wavelength of incident x-ray, θ = Diffraction angle, n = Integer

3.2.2 Differential Thermal Analysis (DTA) / TGA

Differential thermal analysis (or **DTA**) is a thermoanalytic technique, similar to differential scanning calorimetry (DSC). In DTA, the material under study and an inert reference are made to undergo identical thermal cycles, while recording any temperature difference between sample and reference. This differential temperature is then plotted against time, or against temperature (DTA curve or thermogram). Changes in the sample, either exothermic or endothermic, can be detected relative to the inert reference. Thus, a DTA curve provides data on the transformations that have occurred, such as glass transitions, crystallization, melting and sublimation. The area under a DTA peak is the enthalpy change and is not affected by the heat capacity of the sample.

A DTA consists of a sample holder comprising thermocouples, sample containers and a ceramic or metallic block; a furnace; a temperature programmer; and a recording system. The key feature is the existence of two thermocouples connected to a voltmeter. One thermocouple is placed in an inert material such as Al_2O_3, while the other is placed in a sample of the material under study. As the temperature is increased, there will be a brief deflection of the voltmeter if the sample is undergoing a phase transition. This occurs because the input of heat will raise the temperature of the inert substance, but be incorporated as latent heat in the material changing phase.

DTA was performed using a model Diamond Pyris. Samples were heated from room temperature to the desired set point (800 ºC) at 10 ºC per minute and then cooled to room temperature inside the furnace with the same cooling rate 10 ºC per minute in N_2 atmosphere.

3.2.3 Scanning Electron Microscopy (SEM)

Scanning electron microscope (SEM) is an important tool for microstructural analysis. The microstructural characteristic of the sample correlate the effect of different processing condition with properties and behaviour of materials that involves their microstructural changes. The SEM provides information relating to topographical features, morphology, phase distribution, compositional differences, crystal orientation and presence of defects and their location. The strength of SEM lies in its inherent versatility due to the multiple signals generated, simple image formation process, wide magnification range and excellent depth of field. The SEM micrographs could be taken in two modes i.e. secondary emission and back scattered. In the present investigation secondary emission mode was used. Structural analyses were carried out to see the morphological features of grain formation. Grain sizes were also measured directly from the micrographs of the samples as grain size influences the ionic conductivity substantially.

3.2.4 Conductivity Measurement

Conductivity measurements were performed using two probe AC impedance spectroscopy technique. Impedance spectroscopy is essentially a non-destructive technique which can provide information that cannot be obtained by other means. Impedance spectroscopy is a powerful ac measurement technique which has been applied quite successfully to determine a number of important characteristics such as bulk resistivity in case of single crystals and contribution of grain and grain boundary resistance in poly crystalline solid electrolytes. SOFC electrolytes are oxygen ion conductors and can therefore be studied using this technique.

The sintered pellets for conductivity measurement were rubbed gently over fine grit paper in order to ensure that their faces were flat and smooth. Gold was sputter coated onto both faces of each pellet. Now, the pellet was placed into a stainless steel sample holder and the wires were connected to Hewlett Packard 4274A Impedance Analyser. The sample holder was then placed into a vertical tubular furnace. Measurement were taken in air at 30 ºC intervals from 200 ºC-720 ºC, in the frequency range 100Hz-100 k Hz.

Figure 3.2 shows a typical Nyquist plot of Z' as a function of –Z'' for an oxide ion conducting solid electrolyte. The high frequency semi circle represents the bulk resistance of the material. The intercept of the semi circle/sloped line with Z axis is the bulk resistance of the material R used to calculate the bulk conductivity σ, where σ = t/AR where t and A are pellet thickness and electrode/pellet contact surface area respectively. Conductivites (σ) of samples were calculated from impedance spectra and sample geometries. Conductivity activation energies – slopes of Arrheinus plots were obtained by plotting the following equation: $\ln \sigma T = \ln \sigma_o - \frac{E_A}{k_B}\frac{1}{T}$ (3)

where E_A is the activation energy for the transport of oxygen ions, σ_0 is a pre exponential factor, k_B is Boltzmann's constant and T is the temperature.

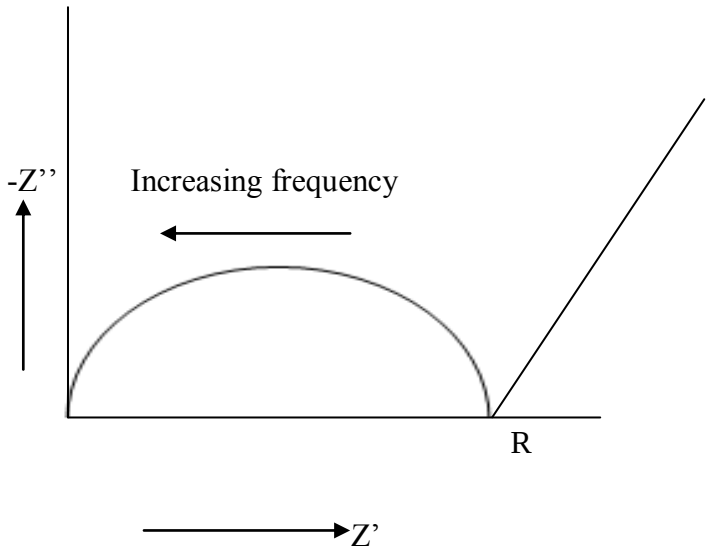

Figure 3.2 Nyquist Plot of Z'as a function of –Z''.

Chapter 4

Results and Discussion

4.1 X-Ray Analysis

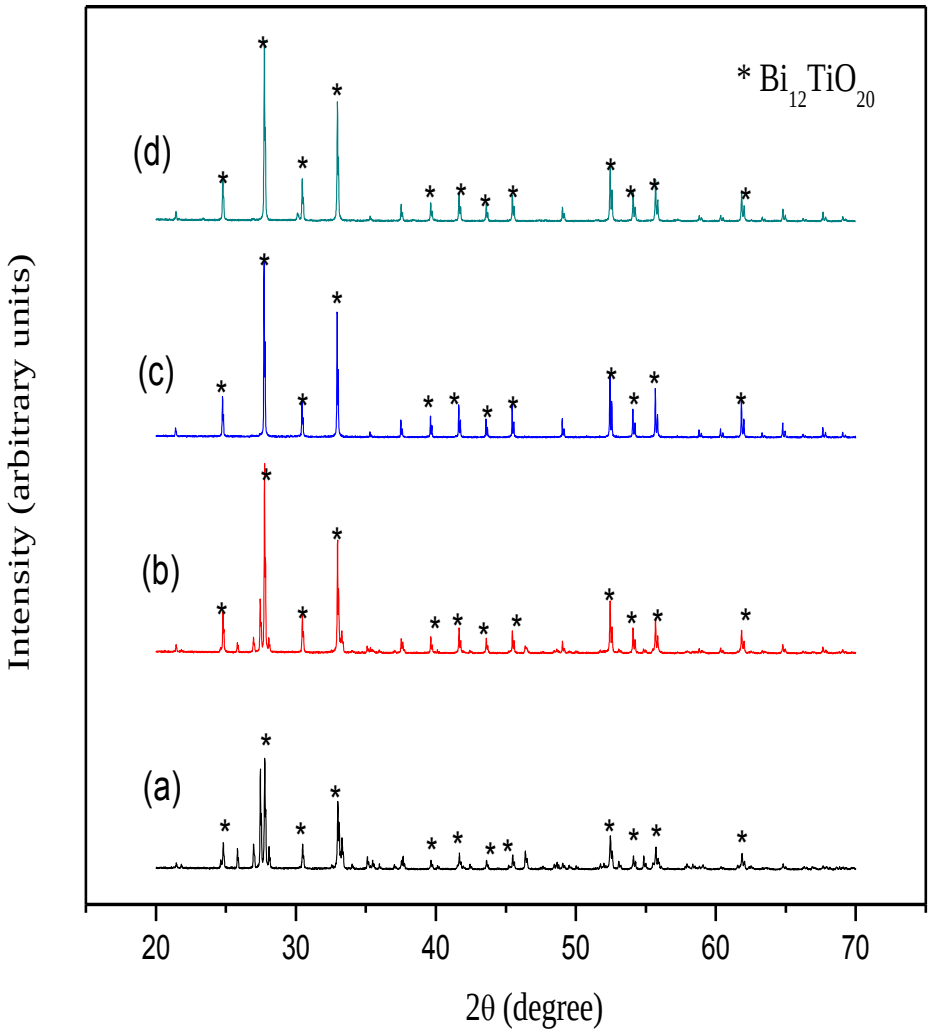

Figure 4.1 X-ray diffraction patterns of $(Bi_2O_3)_{1-x}(TiO_2)_x$ for (a**)** x = 0.05, (b**)** x = 0.10, (c**)** x = 0.15 and (d**)** x = 0.20.

The X-ray powder diffraction data were collected for all samples at room temperature in the range of $20° \leq 2\theta \leq 70°$ at the scan speed of 5°/ min using monochromatic Cu Kα radiation having 1.54 Å wavelength.

X-ray diffraction patterns of TiO_2 doped samples are shown in Figure 4.1a-d. A series of compound having the composition $(Bi_2O_3)_{1-x}(TiO_2)_x$ for x = 0.05, 0.10, 0.15 and 0.20 were characterized by X-ray diffraction using Panalytical. All the four samples exhibited $Bi_{12}TiO_{20}$ cubic phase indexed with ICDD card number (34-0097) with some secondary peak of α-Bi_2O_3 compared with ICDD card number (41-1449) for x = 0.05 and 0.10 indicating the presence of mixed phase as mentioned in the phase diagram given by Shintaro Miyazawa [21]. The lattice constant of $Bi_{12}TiO_{20}$ (10.17391 Å) being about $\sqrt{3}$ times that of δ-Bi_2O_3, (5.66 Å). X-ray diffraction pattern clearly show that the volume fraction of $Bi_{12}TiO_{20}$ phase increases with increasing the mole of TiO_2. The shifting in the XRD peak is due to the strain induced because of the mismatch in the ionic radii of host cation Bi^{3+} (1.03 Å) and dopant cation Ti^{4+} (0.745 Å). Hence, the result of present X-ray study reveal that cubic phase is stabilised in TiO_2 doped samples to room temperature within the range of dopant concentration studied as compared to other dopant oxide like ZrO_2 with Zr^{4+} (r = 0.86 Å) [37] show tetragonal phase and Gd_2O_3 with (r = 0.94 Å) [36] show rhombohedral phase having greater cationic radius than Ti^{4+}. So, by reducing the average cationic radius cubic fluorite bismuth oxide can be stabilized which is reported by other researchers [36, 44].

4.2 Lattice Constant

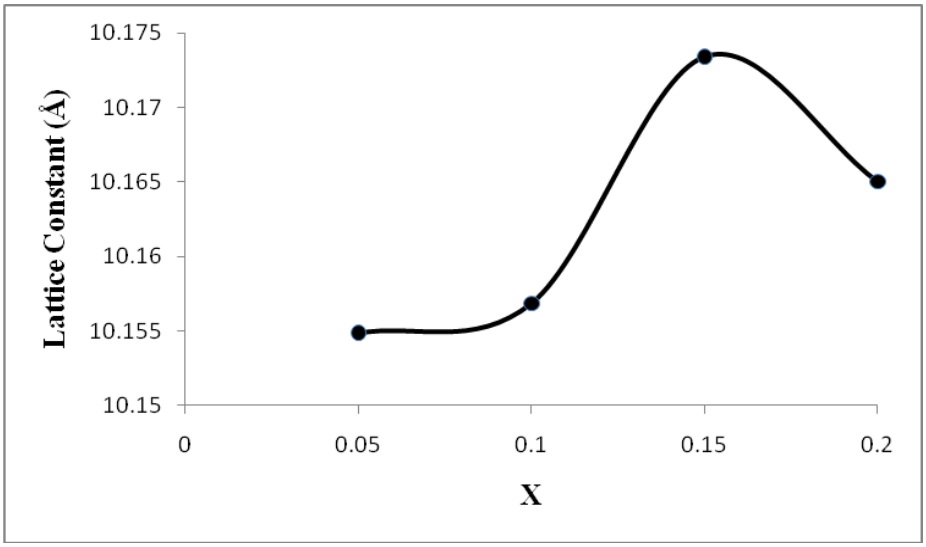

Figure 4.2 Variation of Lattice constant with composition in $Bi_{2-x}TiO_{3+x/2}$.

Figure 4.2 shows the variation of lattice constants as a funciton of TiO_2 concentration. The measurements were carried out for each sample. X-ray diffraction patterns of samples with a TiO_2 of less than the x = 0.15 TiO_2 (hypo-peritectic region) showed the existence of Bi_2O_3 phase. As TiO_2 concentration is increased the lattice constant increases rapidly from x = 0.05 to about a maximum value at around x = 0.15 and then decreases for x = 0.20 (BT4). This results suggests that the solid solution limit lies at round x = 0.15. In other words, the solid solubility limit of x in $(Bi_2O_3)_{1-x}(TiO_2)_x$ system is $0<x<0.15$. It can be readily supposed that there exist a solid solution in the hypo-peritectic region. This non-linear relationship between the solution composition and the lattice constant might be due to the substitution of Bi^{3+} (r = 1.03Å) by smaller Ti^{4+} (r = 0.745Å) and incorporation of additional O^{2-} ions into the vacant sites that result to expand the unit cell as suggested by Abraham *et al.* [37] for dopant ZrO_2 in $Bi_{2-x}Zr_xO_{3+x/2}$ ($0.05\leq x\leq 0.17$) system. So, these two effects suggest that intially the variation in lattice constant is due to second effect with increase in the value of lattice constant for x lie between 0.05 and 0.15 whereas the first affect dominant for x between 0.15 and 0.20.

4.3 Thermal Analysis

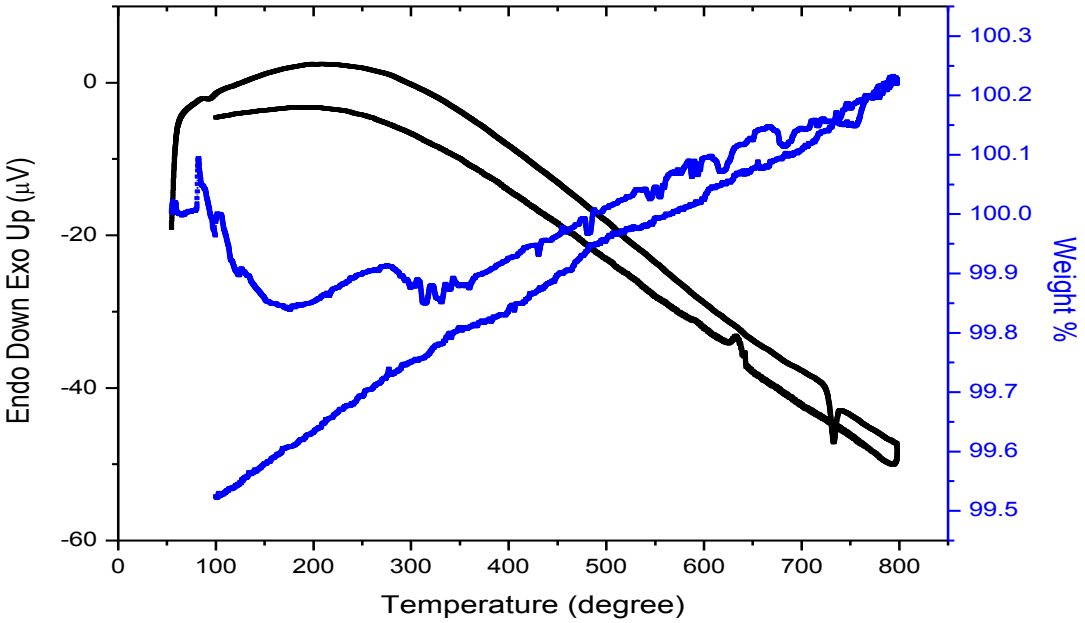

Figure 4.3a DTA/TGA for BT1.

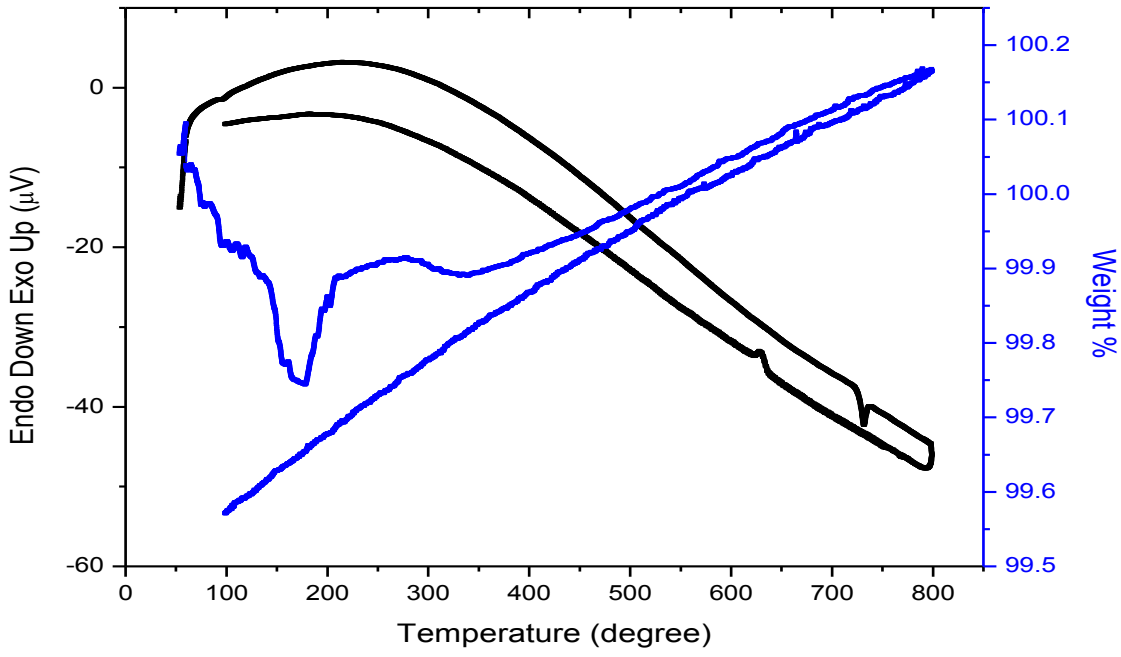

Figure 4.3b DTA/TGA for BT2.

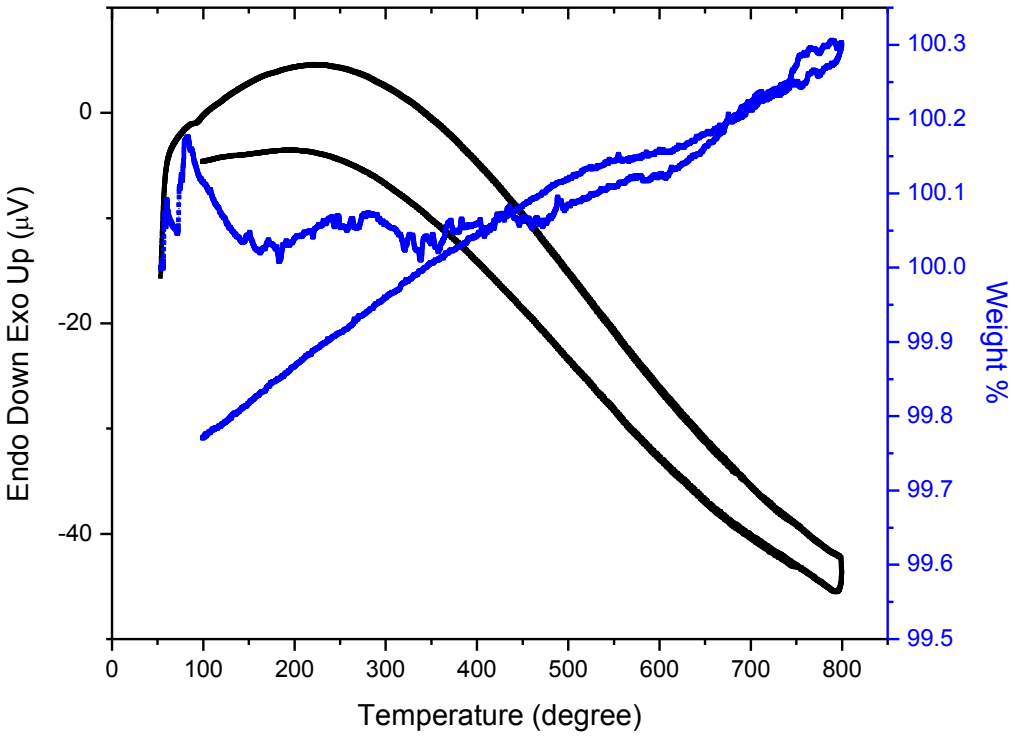

Figure 4.3c DTA/TGA for BT3.

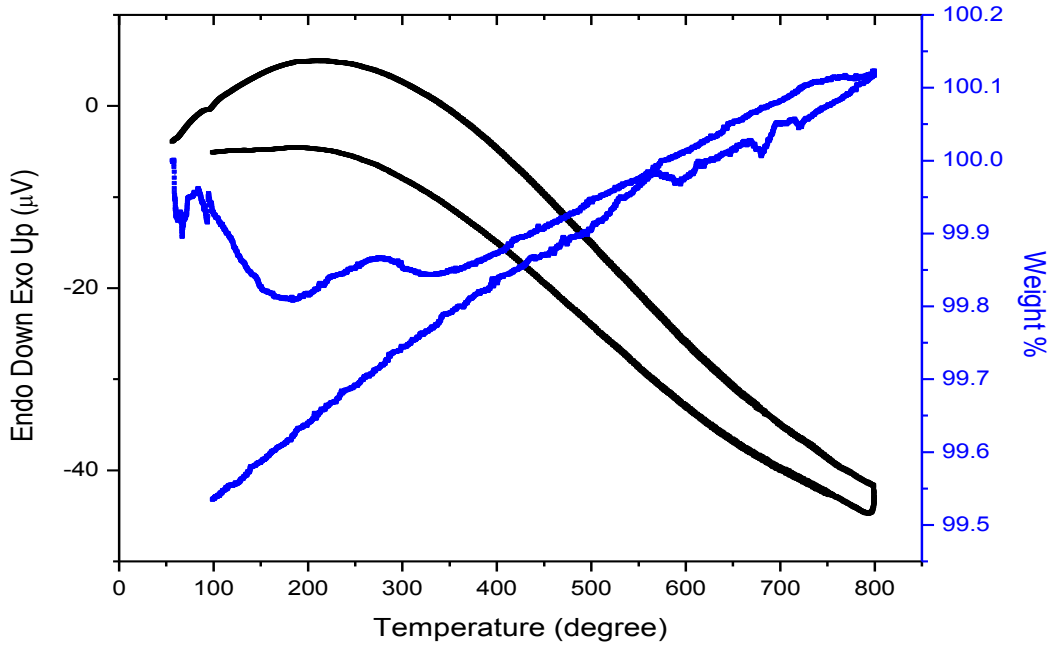

Figure 4.3d DTA/TGA for BT4.

Figure 4.3a-d show differential thermal analysis traces for all composition $0.05 \leq x \leq 0.20$. On heating for x = 0.05 powder mixture exhibit one endothermic heat effect at about 730 ºC which arises from the phase transition of α-Bi_2O_3 to δ-Bi_2O_3 while during cooling two exothermic events are evident: a exotherm at 640 ºC immediately followed by second exotherm at 630 ºC. The first thermal event during cooling is associated with transition of δ-phase to γ-phase at about 640 ºC whereas the second peak corresponds to transformation of γ-phase to β-phase at about 630 ºC. For dopant concentration x = 0.10 only one endothermic heat effect occur at about 731 ºC which corresponds to transformation of α-phase to δ-phase while during cooling one exothermic heat effect occur at about 630 ºC showing the transition of δ-phase to β-phase. For dopant concentration x = 0.15 and x = 0.20 no recognizable heat effect detected during either heating or cooling. This finding confirms that volume fraction of $Bi_{12}TiO_{20}$ phase increases at the cost of α-Bi_2O_3 phase. TG curve reveals a very slow and gradual mass decrease. The observed mass change in the TG curve corresponds to volatilization of the Bi_2O_3.

4.4 Electrical Conductivity

Impedance spectra were used to determine the electrical properties of the material synthesized by solid state method. Selected impedance spectra recorded in the temperature range 200 ºC-750 ºC and in the frequency range from 100 Hz-100 kHz are shown in Figure 5.4.

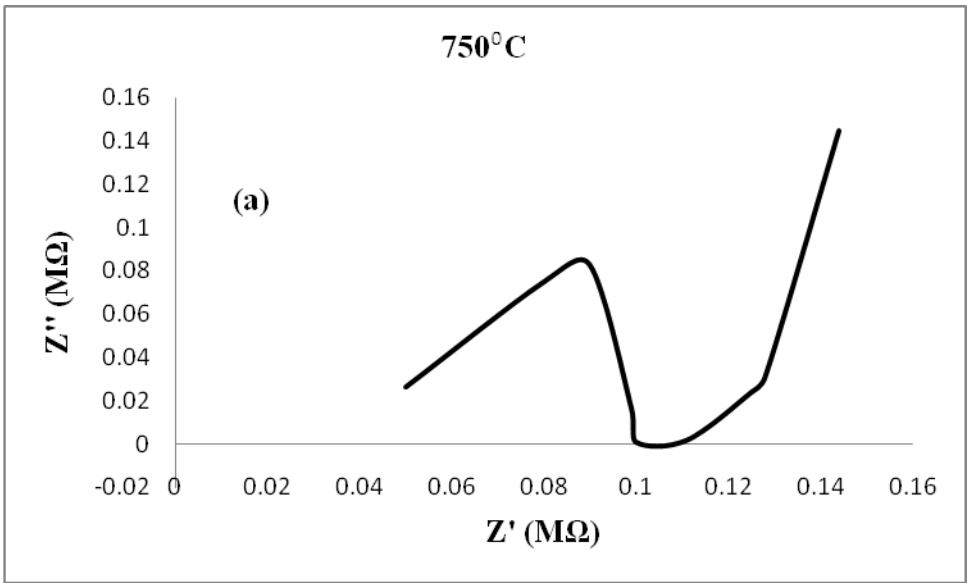

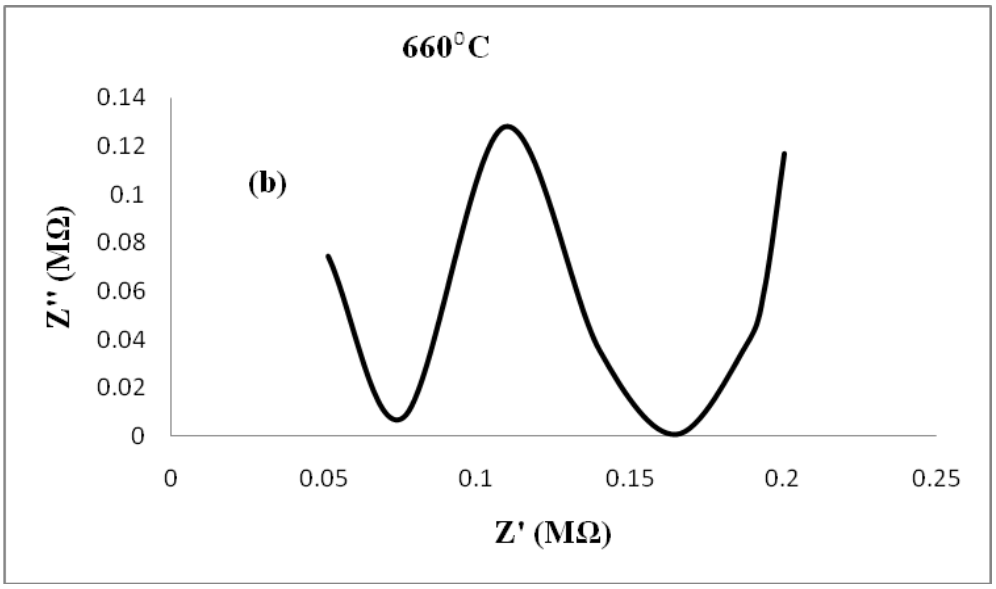
660°C
(b)
Z'' (MΩ)
0.14
0.12
0.1
0.08
0.06
0.04
0.02
0
0
0.05
0.1
0.15
0.2
0.25
Z' (MΩ)

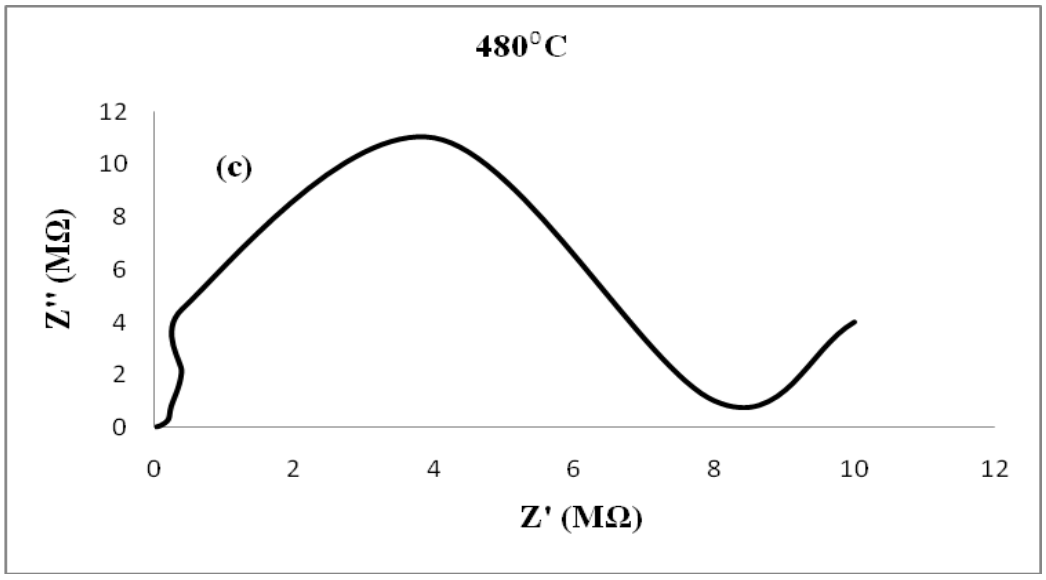
480°C
(c)
Z'' (MΩ)
12
10
8
6
4
2
0
0
2
4
6
8
10
12
Z' (MΩ)

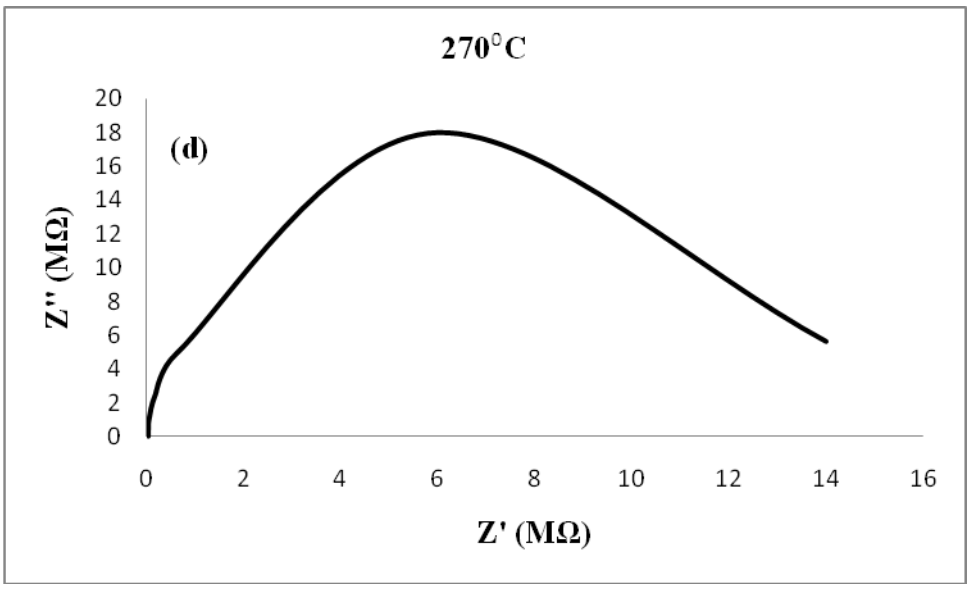
270°C
(d)
Z'' (MΩ)
20
18
16
14
12
10
8
6
4
2
0
0
2
4
6
8
10
12
14
16
Z' (MΩ)

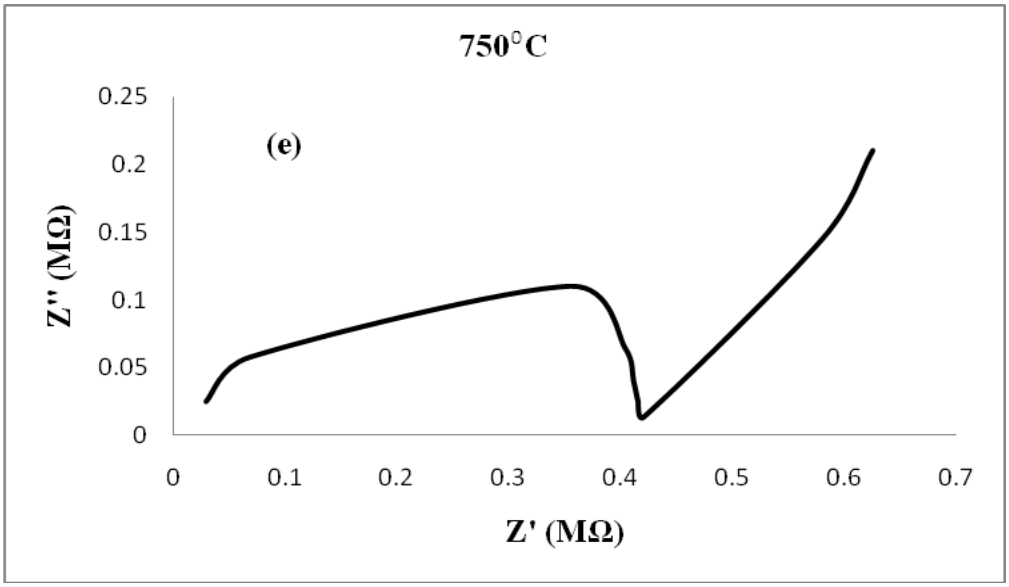
750°C
(e)
Z'' (MΩ)
0.25
0.2
0.15
0.1
0.05
0
0
0.1
0.2
0.3
0.4
0.5
0.6
0.7
Z' (MΩ)

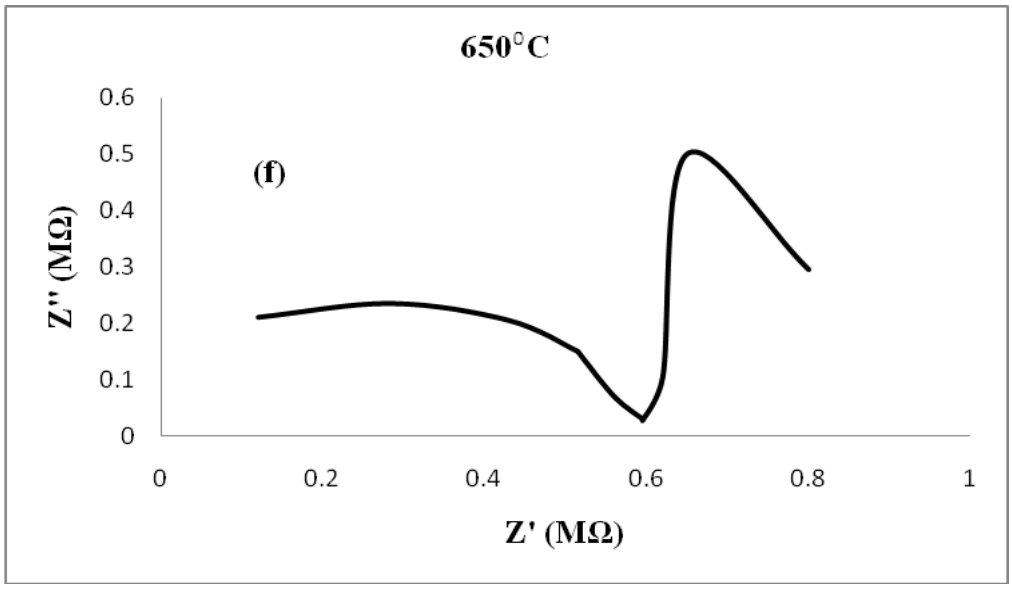
650°C
(f)
Z'' (MΩ)
0.6
0.5
0.4
0.3
0.2
0.1
0
0
0.2
0.4
0.6
0.8
1
Z' (MΩ)

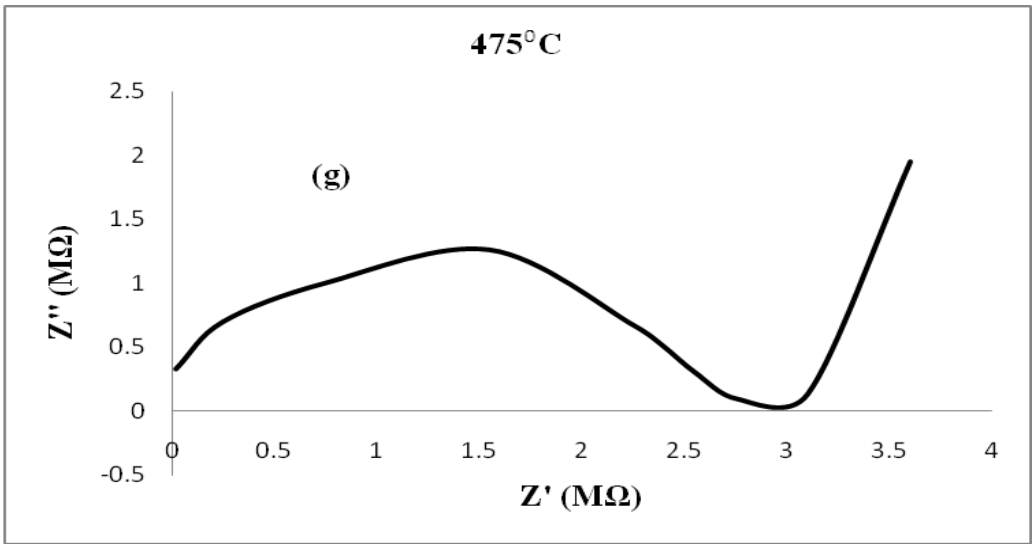
475°C
(g)
Z'' (MΩ)
2.5
2
1.5
1
0.5
0
-0.5
0
0.5
1
1.5
2
2.5
3
3.5
4
Z' (MΩ)

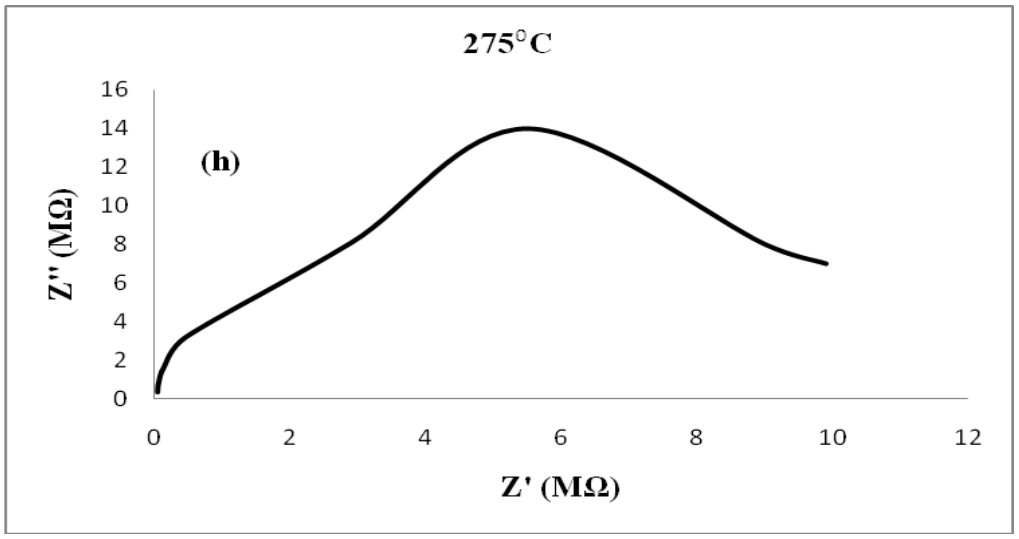

Figure 4.4 Selected Impedance plot measured at different temperature of the solid solution $(Bi_2O_3)_{1-x}(TiO_2)_x$ for (a)-(d) x = 0.15 and (e)-(h) x = 0.20

With increasing temperature from 200 ºC-750 ºC the resistivity of the sample-to-electrode had greater influence on the overall sample resistivity. The bulk resistivity is equal to the sum of the grain and grain boundary resistivities. Although at low temperature Bi_2O_3 has a significant electronic contribution to total conductivity. It is assumed that as in pure Bi_2O_3 the high temperature conductivity is mainly ionic.

The Arrhenius plots of total conductivity for composition $(Bi_2O_3)_{1-x}(TiO_2)_x$ (x = 0.05, 0.15 and 0.20) shown in Figure 4.5.

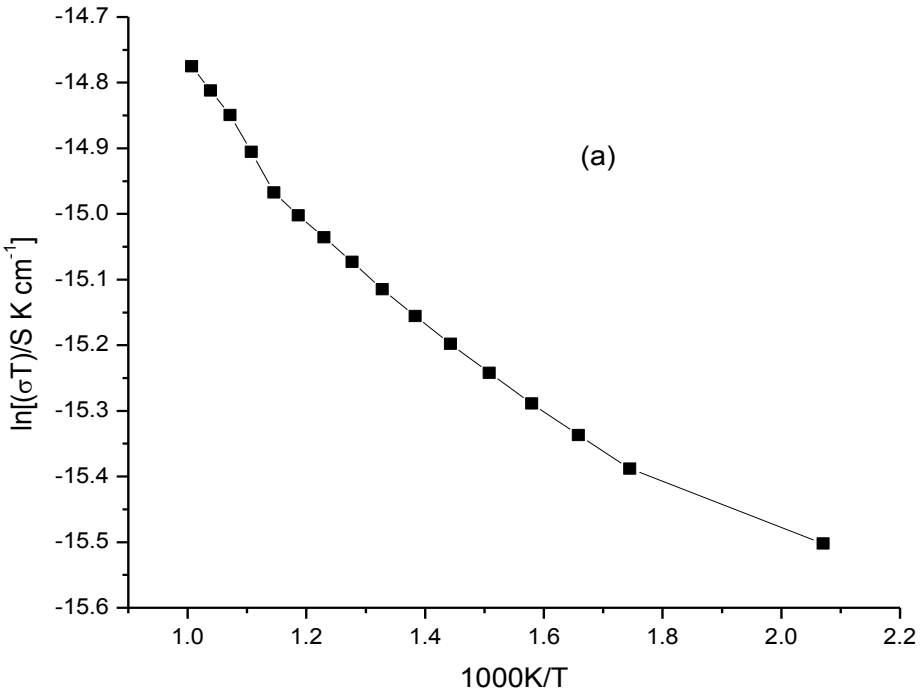
(a)
ln[(σT)/S K cm-1]
-14.7
-14.8
-14.9
-15.0
-15.1
-15.2
-15.3
-15.4
-15.5
-15.6
1.0
1.2
1.4
1.6
1.8
2.0
2.2
1000K/T

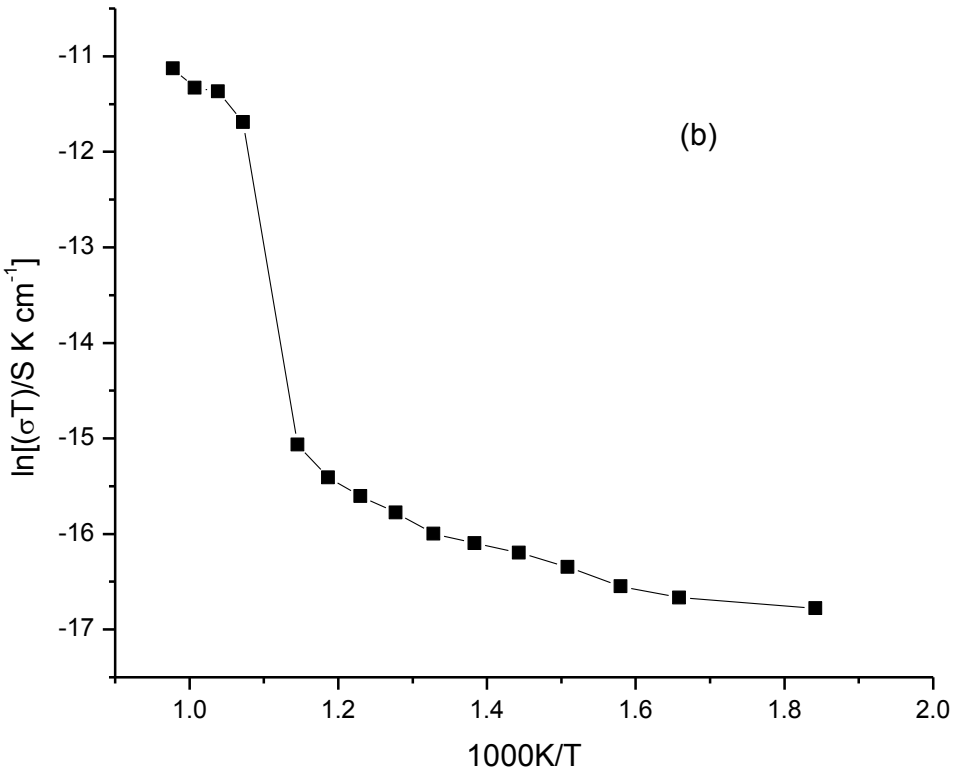
(b)
ln[(σT)/S K cm-1]
-11
-12
-13
-14
-15
-16
-17
1.0
1.2
1.4
1.6
1.8
2.0
1000K/T

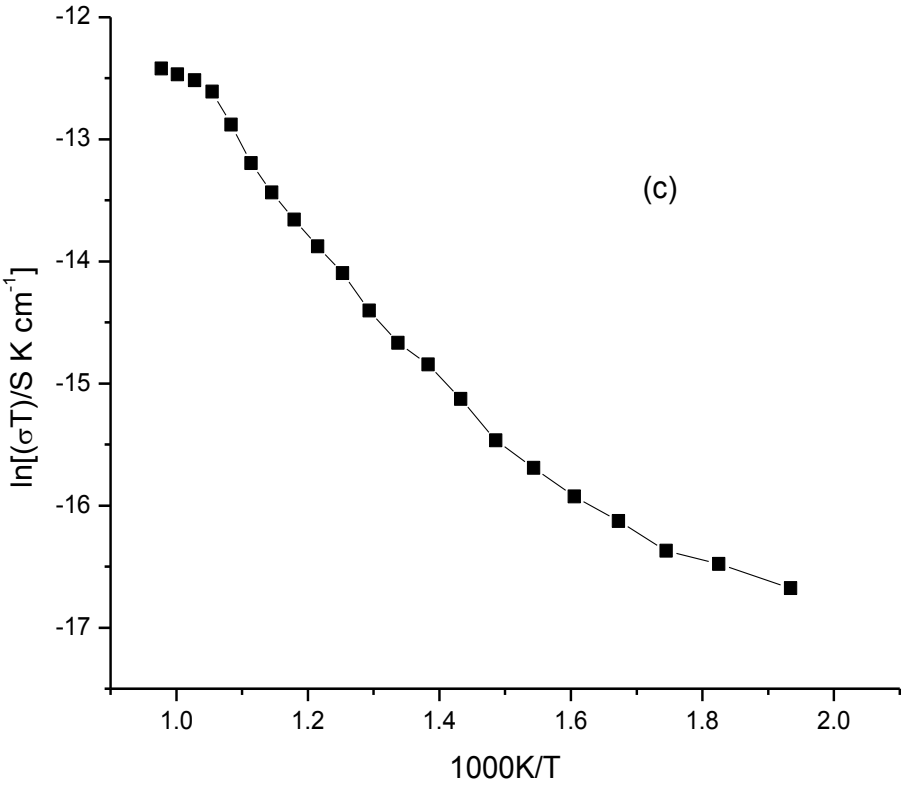

Figure 4.5 Arrhenius plot of conductivity for (a) x = 0.05, (b) x = 0.15 and (c) x = 0.20 over cooling cycles.

Each conductivity plot can be divided into two linear regions one at low temperatures and one at high temperatures for x = 0.15 and x = 0.20. The separation of the regions occurs at about 660 ºC for x = 0.15 and 675 ºC for x = 0.20. This discontinuity in the cooling cycle for both composition values has been attributed to small changes in oxygen stoichiometry. The conductivity data for all composition are summarised in Table VI.

Table VI Conductivity parameter for composition in the $(Bi_2O_3)_{1-x}(TiO_2)_x$ system

x	300 °C		650 °C	
	σ (S cm^{-1})	**ρ (Ω cm)**	**σ (S cm^{-1})**	**ρ (Ω cm)**
0.00	-	-	1 [12]	1
0.05	3.6×10^{-10}	2.76×10^{9}	3.8×10^{-10}	2.62×10^{9}
0.15	4.8×10^{-10}	2.08×10^{9}	9.0×10^{-9}	1.11×10^{8}
0.20	1.3×10^{-10}	7.36×10^{9}	2.7×10^{-9}	3.6×10^{8}

The high temperature conductivity measured at 650 °C (σ_{650}) shows a drop in conductivity when compared to the literature value for the pure Bi_2O_3 system rise with increasing Ti content to reach at maximum 9×10^{-9} S cm^{-1} and then decrease with increasing Ti content to return value of 2.7×10^{-9} S cm^{-1} at the $(Bi_2O_3)_{1-x}(TiO_2)_x$ composition. The decrease in conductivity at high temperature might be explained as a defect trapping effect. It is known that grain boundary effects are more significant factor at low temperature than at high temperature. Grain boundaries have an important effect on the overall conductivity and grain boundary is affected by factors such as grain size and impurity level among others. Impurities including a second phase introduced by the starting materials or during the fabrication procedure affect the ionic conductivity because they tend to accumulate at grain boundary during sintering. Various studies have shown that these phases suppress grain growth, resulting in small grain size and larger grain boundary volume fraction. These impurities provide a blocking layer within the grain boundary that makes the grain boundary less conductive and reduce the total conductivity. So, the presence of secondary phase Bi_2O_3 may affect the conductivity which decreases with increasing the dopant concentration. Since, at high temperature grain boundary effect is less so the drop in conductivity observed at high temperature must be due to defect trapping effect which can be characterised due to strong association of the oxygen vacancies with the small Ti^{4+} ions. Decreases in mobile oxygen vacancies and a subsequent drop in conductivity are expected because Ti ions are able to trap oygen vacancy more effectively [49]. This is also consistent with the fact the conductivity in cubic bismuth oxides is reduced due to the substitution of highly polarizable bismuth ions with less polarizable Ti^{4+} ions in the cation sublattice. Because polarizability is proportional the cube of ionic radius [6] and Ti^{4+} (r = 0.745 Å) is

smaller than Bi^{3+} (r = 1.03 Å). So, the ionic conductivity of doped cubic bismuth oxide decreases with incresing dopant concentration of less polarizable Ti^{4+}.

4.5 SEM observation

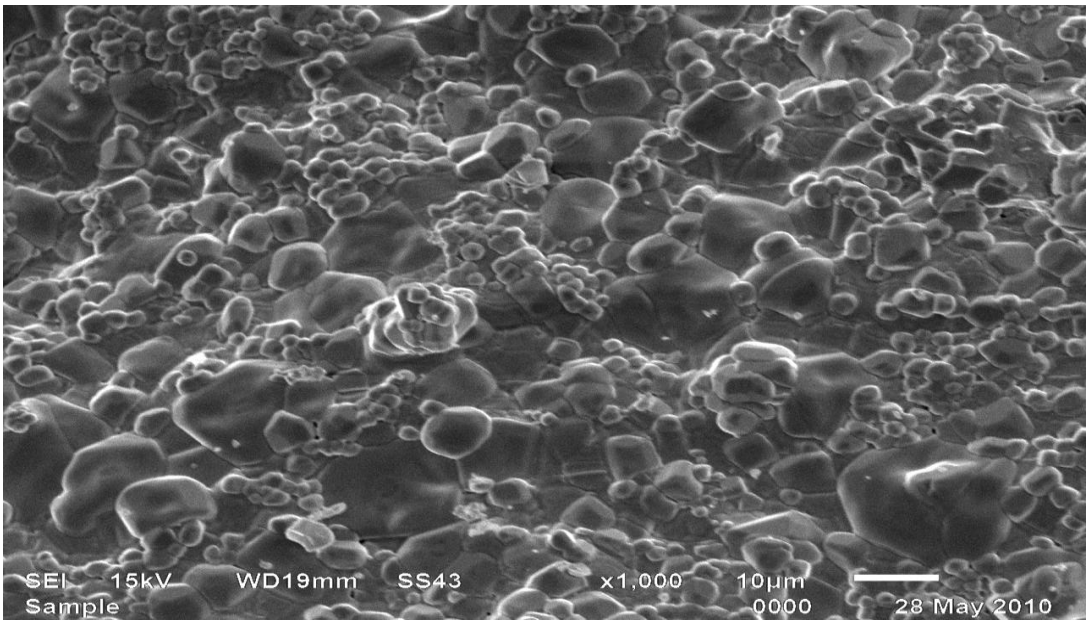

Figure 4.6a. SEM image BT2 at 1000× magnification.

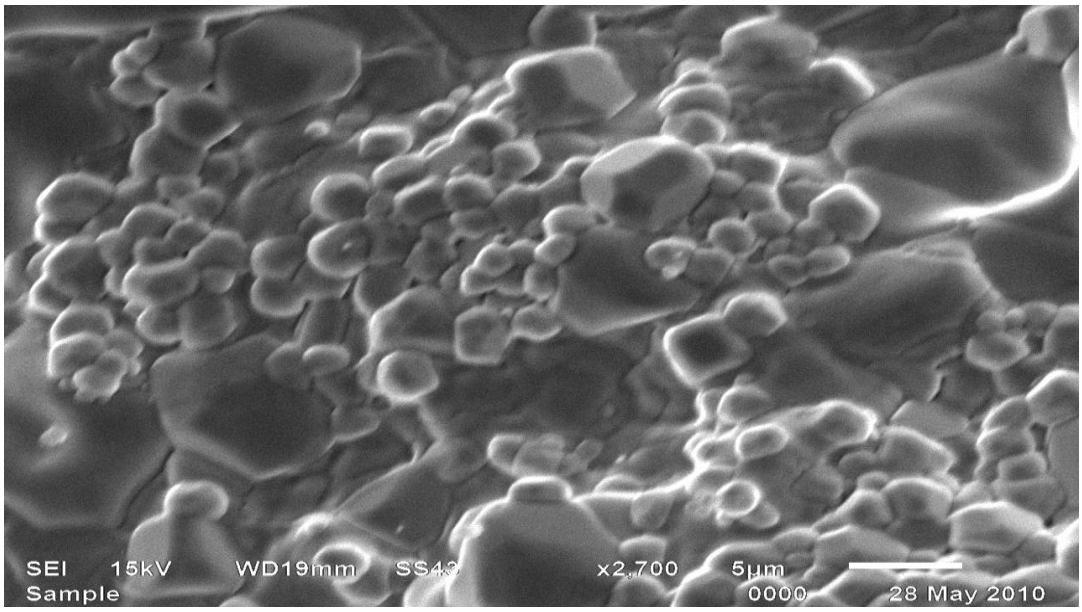

Figure 4.6b. SEM image for BT2 at 2700× magnification.

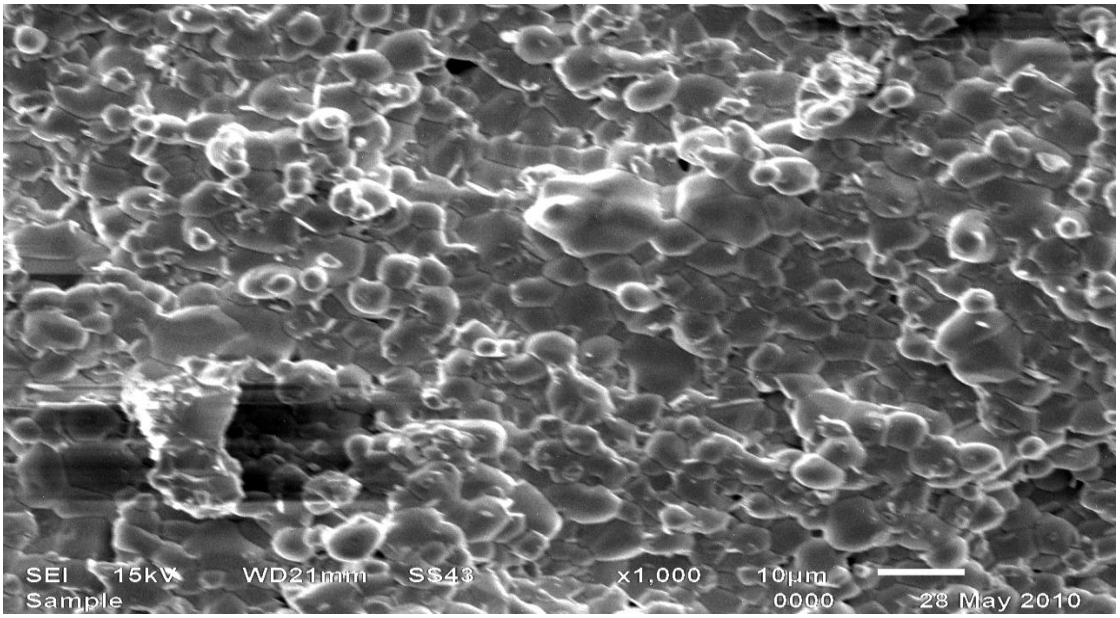

Figure 4.6c. SEM image for BT3 at 1000× magnification.

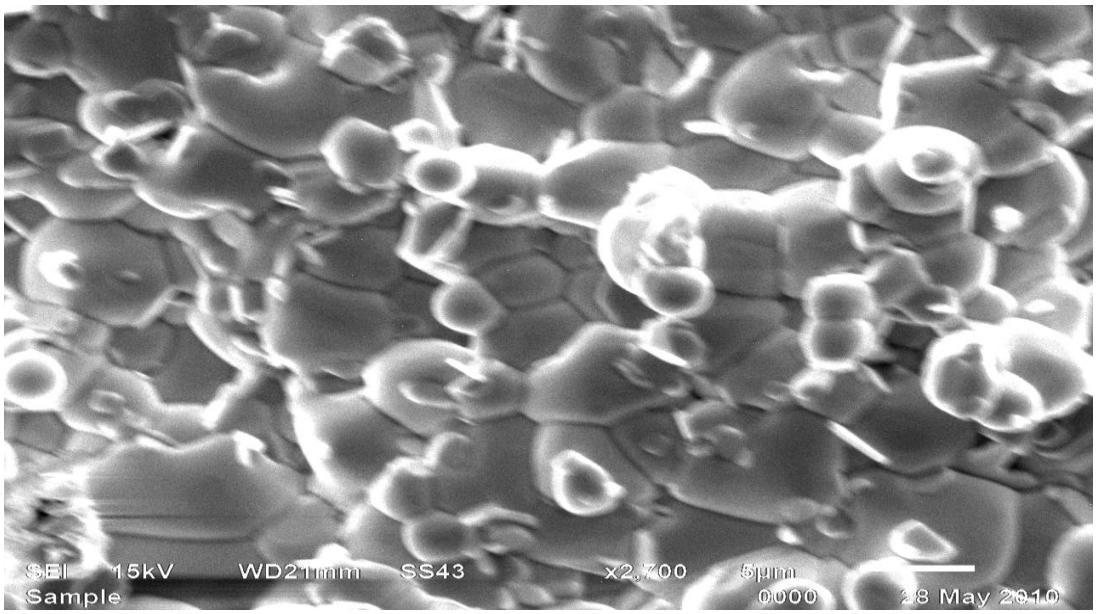

Figure 4.6d. SEM image for BT3 at 2700× magnification.

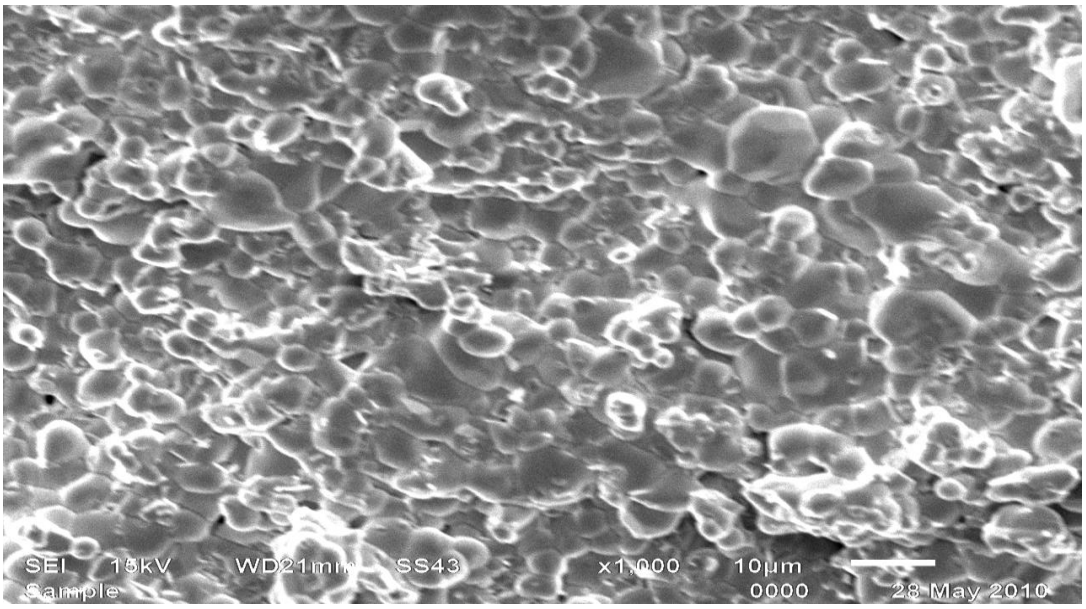

Figure 4.6e. SEM image for BT4 at 1000× magnification.

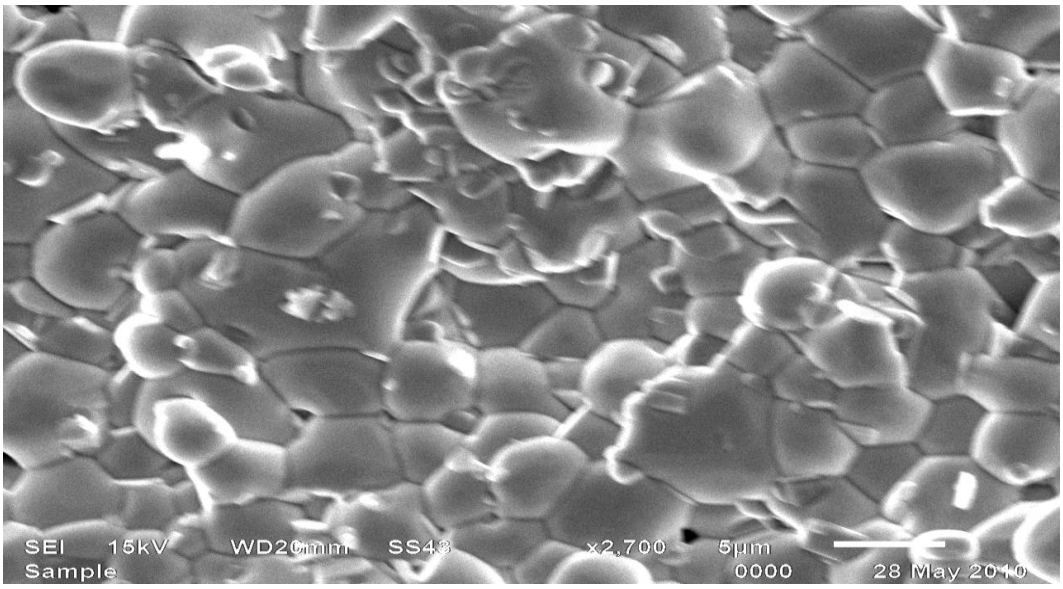

Figure 4.6f. SEM image for BT4 at 2700× magnification.

To verify the results of XRD, the microstructure of fractured surface was further examined by SEM. Figure 4.6a-f shows the SEM micrograph of composition $(Bi_2O_3)_{1-x}(TiO_2)_x$ for x = (a)-(b) 0.10, (c)-(d) 0.15 and (e)-(f) 0.20. The SEM clearly show that $(Bi_2O_3)_{1-x}(TiO_2)_x$ (x = 0.10, 0.15 and 0.20) are composed of two phases. Two types of grains are clearly observed as shown in Figure 4.6a-f. The amount of cubic $Bi_{12}TiO_{20}$ phase which is responsible for conductivity is, more for x = 0.15 and x = 0.20. The circle like grains appeared which decreases with increasing amount Ti ion content.

Therefore, it is suggested that composition of circle like grains corresponds to second phase. The conductivity of sample for x = 0.10 is on lower side than for x = 0.15 and x = 0.20 because of the presence of second phase in observed in high amount which support the result of XRD analysis as shown in Figure 4.1.

Chapter 5

Conclusion and Future Scope

The as-sintered $(Bi_2O_3)_{1-x}(TiO_2)_x$ (x = 0.05, 0.10, 0.15 and 0.20) samples exhibit cubic $Bi_{12}TiO_{20}$ phase with very small amount of Bi_2O_3 as clearly indicated from SEM and XRD analysis. XRD and SEM analysis suggests that secondary phase decrease with increasing dopant concentration and cubic phase stabilised because of the substitution of Bi^{3+} (r=1.03 Å) by smaller Ti^{4+} (r=0.745 Å). According to DTA result the composition $(Bi_2O_3)_{1-x}(TiO_2)_x$ was stable on heating and cooling between room temperature and 800 ^{0}C for x=0.15 and x=0.20. This indicated that x=0.15 and x=0.20 samples makes stable solid solution with low ionic conductivity. The highest conductivity is observed for x=0.15 is 9×10^{-9} S cm^{-1} which is lower than pure δ-Bi_2O_3. The reason of lower conductivity might be attributed due to the presence of secondary phase which segregate along the grain boundary and reduce the ionic conductivity. SEM results also clearly indicates that in BT2, BT3 and BT4 samples, minor α-Bi_2O_3 phase segregates along the grain boundaries. Additionally, the well sintered and clear grains are also observed in BT3 and BT4 samples as compared to BT2 sample. On the other hand, $Bi_{12}TiO_{20}$ cubic phase is present in large amount in BT3 and BT4 samples which is responsible for higher ionic conductivity than BT2 sample. But at high temperature grain boundary effect is not prominent. So, at high temperature the trapping of the oxygen vacancy by Ti^{4+} ions reduces the ionic conductivity. One more supporting fact to this lower conductivity in cubic bismuth oxide is the substitution of highly polarizable bismuth ions with less polarizable Ti^{4+} ions in the cation sublattice.

Future Scope

The mechanical properties and thermal expansion coefficient of these samples can be investigated which can be improved by doping different cations without degrading the ionic conductivity. Also, this foreign cations should be those which minimize the ionic radius mismatch between Bi and Ti ions into the cations sublattice of $(Bi_2O_3)_{1-x}(TiO_2)_x$. Also, the solid solution limit can be investigated by increasing the value of x or by taking small interval value of x (nearly$\leq$0.025) in $(Bi_2O_3)_{1-x}(TiO_2)_x$ system which is around about x=0.15.

References:-

[1] T. Takahashi, H. Iwahara and Y. Nagai, *J. Appl. Electrochem*, **2** (1972): p. 97.

[2] F. Abraham, J. C Baivin, G. Mairesse and G. Mowogrocki, *Solid State Ionics*, **40/41** (1990): p. 934.

[3] Thanganathan Uma and Masayuki Nogami, *Jpn. Anal. Chem.*, **80(2)** (2008): p. 506–508.

[4] Jungho Ryu, Hyeoung Woo Kim, Kenji Uchino and Jaehyung Lee, *Jpn. J. Appl. Phys.*, **42** (2003): p. 1307-1310.

[5] T. Takahashi and H. Iwahara, *J. Appl. Electrochem.*, **3** (1973): p. 65.

[6] Eric D. Wachsman, Sai Boyapati and Naixiong Jiang, *Solid State Ionics*, **7** (2001): p. 1-5.

[7] E. M. Levin and R. S Roth, *J. Res. Natl. Bur. Stand.*, **68A** (1964): p. 197.

[8] M. Drache, P. Rousel and J. P. Wignacourt, *Chem. Rev.*, **107** (2007): p. 80.

[9] H. A Harwig and A. G Gerads, *J. Solid State Chem.*, **26** (1978): p. 265.

[10] P. D Battle, R. A Catlow, J. W Heap and L. M Moroney, *J. Solid State Chem.*, **63 (**1998): p. 8.

[11] T. Takahashi, H. Iwahara and T. Nagal, *J. Appl. Electrochem.*, **2 (**1972): p. 97.

[12] A. Laarif and F. Theobald, *Solid State Ionics*, **21** (1986): p. 183.

[13] G. Mairesse, B. Scrosati, A. Magistris, C. M Mari and G. Mariotto (Eds.), *Kluver Academic Publishers Dordrecht*, (1993): p. 271.

[14] L. E Smart and E. A Moore, *Solid State Chemistry*, (2005): p. 183.

[15] J. C Boivin and G. Mairesse, *Chem. Mater.*, **10** (1998): p. 2810.

[16] J. Y Park, H. Yoon and E. D Wachsman, *J. Am. Ceram. Soc.*, **88** (2005): p. 2402.

[17] R. D Shannon, *Acta Crystallogr.*, **A32** (1976): p. 751.

[18] Feng-Yun Wang, Songying Chen and Soofin Cheng, *Electrochem. Commun.*, **6** (2004): p. 743–746.

[19] F. Abraham, A. F. Debreuille-Gresse, G. Mairesse and G. Nowogrocki, *Solid State Ionics*, **28-30** (1988): p. 529.

[20] O. H. Kwon and G. M. Choi, *Solid State Ionics*, **177** (2006): p. 3057–3062.

[21] Shintaro Miyazawa, *J. Korean Association of Crystal Growth*, **9(4)** (1999): p. 424-431.

[22] N. Jiang and E. D Wachsman, *J. Am Ceram Soc.*, **82** (1999): p. 3057.

[23] D. S Aidhy, J. C Nino, S. B Sinnott, E. D Wachsman and S. R Phillpot, *J. Am Ceram Soc.*, **91** (2008): p. 2349.

[24] S. Dilpuneet, B. Aidhy, Susan. Sinnott, E. D. Wachsman and Simon R. Phillpot, *Solid Statec Ionics*, **16** (2010): p. 297–303.

[25] V. M. Zaĭnullina and V. P. Zhukov, *Phys. Solid State*, **43(9)** (2001): p. 1686–1699.

[26] John B. Goodenough, *Annu. Rev. Mater. Res.*, **33** (2003): p. 91–128.

[27] V. P. Zhukov, V. M. Zhukovskii, V. M. Zainullina, and N. I. Medvedeva, *J. Struct. Chem.*, **40(6)** (1999): p. 831-837.

[28] M. Mohri, Y. Tajima, H. Tanaka, T. Yoneda, S. Satoh and M. Kasahara, *J. Sharp Tech.*, **34** (1986): p. 97.

[29] M. J. Verkerk and A. J. Burggraaf, *J. Electrochem. Soc.*, **128** (1981): p. 75.

[30] J. M Amarilla and R. M Rojas, *Chem. Mater.*, **8** (1996): p. 401-407.

[31] J. Yan and M. Greenblatt, *Solid State Ionics*, **81** (1995): p. 225.

[32] J. Chmielowiec, G. Pasciak and P. Bujlo, *Mater. Sci.*, **27** (2009): p. 1251-1256.

[33] Ravi Kant, K. Singh and O. P. Pandey, *Solid State Ionics*, **15** (2009): p. 567-570.

[34] Ravi Kant, K. Singh and O. P. Pandey, *Solid State Ionics*, **16** (2010): p. 277-282.

[35] F. Krok, I. Abrahams, M. Malya, W. Bogusz and J. A. G Nelstrop, *Solid State Ionics*, **3** (1997): p. 237.

[36] Srikant Ekhelikar and G. K Bichile, *Bull Mater Sci.*, **27** (2004): p. 22.

[37] I. Abrahams, A. J Bush, S. C. M. Chan, F. Krok and W. Wrobel, *J. Mater. Chem.*, **11** (2001): p. 1715-1721.

[38] I. De Meatza, J. P Chapman, F. Mauvy, J. I. De Larramendi, M. I. Arriortua and T. Rojo, *Mater. Res. Bull.*, **39** (2004): p. 1841-1847.

[39] Čedomir Jovalekić, Miodrag Zdujić, Dejan Poleti, Ljiljana Karanović and Miodrag Mitrić, *J. Solid State Chem.*, **181** (2008): p.1321-1329.

[40] Kapil Sood, Kulvir Singh and O. P. Pandey, *Solid State Ionics*, (2010).

[41] Jun-Young Park, Heesung Yoon and Eric D. Wachsman, *J. Am. Ceram. Soc.*, **88(9)** (2005): p. 2402-2406.

[42] Miodrag Zdujić, Dejan Poleti, Čedomir Jovalekić and Ljiljana Karanović, *J. Serb. Chem. Soc.*, **74(12)** (2009): p. 1401-1411.

[43] S. N. Ng, Y. P tan and Y. H Taufiq-Yap, *J. Phy. Sci.*, **20(1)** (2009): p. 75-86.

[44] Cheng-Yen Hsieh and Kuan-Zong Fung, *J. Solid State Electrochem.*, **13** (2009): p. 951-957.

[45] M. H. Paydar, A. M. Hadian, K. Shimanoe and N. Yamazoe, *J. Mater. Sci.*, **37** (2002): p. 2273-2278.

[46] S.C. Singhal and K. Kendall, *High-temperature Solid Oxide Fuel Cells: Fundamentals, Design and Applications*, (2004).

[47] Swadesh Kumar Pratihar, *Solid oxide fuel cell*, (2008).

[48] S. C. Sinhal, *Solid State Ionics*, **152–153** (2002): p. 405–410.

[49] A. Kaiser, A. J. Feighery, D. P. Fagg and J. T. S. Irvine, *Solid State Ionics*, **4** (1998): p. 218.